



EUROPEAN  
COMMISSION

European  
Research Area

# Carbon-14 Source Term

## CAST



<sup>14</sup>CAST

## 1<sup>st</sup> Annual WP3 Progress Report (D3.5)

Author(s):

**Sophia NECIB,**

David BOTTOMLEY, Crina BUCUR, Nadège CARON, Florence COCHIN, Manuela FULGER, Jean-Marie GRAS, Michel HERM, Viktor JOBBAGY, Volker METZ, Tomofumi SAKURAGI, Tomo SUZUKI-MURESAN, Hiromi TANABE

Date of issue of this report: 01/12/2014

The project has received funding from the European Union's European Atomic Energy Community's (Euratom) Seventh Framework Programme FP7/2207-2013 under grant agreement no. 604779, the CAST project.

### Dissemination Level

<b>PU</b>	Public	<b>x</b>
<b>RE</b>	Restricted to the partners of the CAST project	
<b>CO</b>	Confidential, only for specific distribution list defined on this document	





## ***CAST – Project Overview***

The CAST project (CARbon-14 Source Term) aims to develop understanding of the potential release mechanisms of carbon-14 from radioactive waste materials under conditions relevant to waste packaging and disposal to underground geological disposal facilities. The project focuses on the release of carbon-14 as dissolved and gaseous species from irradiated metals (steels, Zircalloys), irradiated graphite and from ion-exchange materials as dissolved and gaseous species.

The CAST consortium brings together 33 partners with a range of skills and competencies in the management of radioactive wastes containing carbon-14, geological disposal research, safety case development and experimental work on gas generation. The consortium consists of national waste management organisations, research institutes, universities and commercial organisations.

The objectives of the CAST project are to gain new scientific understanding of the rate of re-lease of carbon-14 from the corrosion of irradiated steels and Zircalloys and from the leaching of ion-exchange resins and irradiated graphites under geological disposal conditions, its speciation and how these relate to carbon-14 inventory and aqueous conditions. These results will be evaluated in the context of national safety assessments and disseminated to interested stakeholders. The new understanding should be of relevance to national safety assessment stakeholders and will also provide an opportunity for training for early career researchers.

For more information, please visit the CAST website at:

<http://www.projectcast.eu>

CAST		
Work Package: 3	CAST Document no. :	Document type:
Task: 3.3	CAST-2014-D3.5	R = report
Issued by: Andra		Document status:
Internal no: DRPFSCM140008		Final

Document title
1 <sup>st</sup> Annual WP3 Progress Report

## Executive Summary

Work Package 3 (WP3) is related to Zircaloy in the CAST project. It aims to better understand C-14 behaviour in waste Zr fuel claddings under disposal conditions with regard to C-14 inventory (and origins), release from waste packages and speciation of released C-14. In order to achieve these objectives, WP3 has been divided into four tasks (from 3.1 to 3.4) and 20 deliverables (from D3.1 to D3.20).

Task 3.1 is devoted to the State of the Art, Task 3.2 focus on analytical development, Task 3.3 aims to characterise the C-14 inventory and C-14 release from leaching experiments and corrosion experiments in alkaline media representative of disposal conditions. Finally Task 3.4 will summarise and synthetise the work performed during the previous Tasks.

During the first year of the CAST project, WP3 participants have worked on Tasks 3.1, 3.2 and 3.3. In total four deliverables have been submitted and are available on the CAST website. For Task 3.1, deliverable 3.1 presents the State of the Art. The review pointed out:

- The importance of N as a precursor of C-14,
- The impact of burn – up (BU) on corrosion of Zircaloy,
- The influence of the Zircaloy type on BU and therefore the thickness of oxide layer,
- The types of corrosion (mainly general corrosion) expected in repository conditions for Zircaloy

- The role of hydrides on corrosion, especially the need to consider transportation in dry casks,
- The corrosion kinetics laws of Zircaloy in water and alkaline media,
- The limits of the corrosion models at high temperature used to extrapolate the corrosion rate of Zircaloy at low temperature. This has been highlighted in water and alkaline media,
- The need to carry out experiments on Zircaloy with a significant oxide thickness ( $>2.5\mu\text{m}$ ),

WP3 participants have worked on Task 3.2 to determine possible analytical techniques to measure C-14 inventory and speciation. The main technique envisaged is LSC (Liquid Scintillation Counting). If this is not sufficiently accurate, AMS will be used as it has a lower detection limit. Spectroscopic methods such as Infra-red will be used to identify the main families of chemical functions (carboxylic acids, aromatic compounds, ketones, alcohols...). Chromatographic techniques will be used to detect and quantify families of molecules.

For Task 3.3, WP3 participants have planned the future experimental work to be performed over the next few years of the CAST Project. They will work on both non-irradiated and irradiated Zr alloys. They have discussed the potential reference leaching solution representative of alkaline media under disposal conditions. In July 2014, it was decided to use a portlandite solution ( $\text{Ca}(\text{OH})_2$ , pH 12.5 at room temperature and  $80^\circ\text{C}$ ). Nevertheless recent calculations revealed that calcite precipitation was likely to occur under the reference conditions, prohibiting optimal C-14 inventory measurements. Consequently the use of  $\text{Na}(\text{OH})$  solution is under discussion to determine its suitability towards the objectives of WP3. The reference time duration has been set at one year, although a few teams will perform intermediate samplings. One team will perform digestion experiments in acidic media ( $\text{H}_2\text{SO}_4/\text{HF}$ ) to measure total C-14 inventory on irradiated  $\text{Zr}_4$ , while the other teams will work on the reference solution.



Corrosion experiments will be performed on both non-irradiated and irradiated Zr, in the reference solution. Gravimetric measurements, electrochemical measurements (Linear Polarisation Resistance (LPR)) and hydrogen measurements techniques will be carried out to measure the low corrosion rates expected (<10nm/yr).



## List of Contents

Executive Summary	i
List of Contents	v
1 Introduction	1
2 Progress	1
2.1 Andra contribution in WP3	1
2.1.1 Inventory and distribution of <sup>14</sup> C in Zircaloy cladding	2
2.1.2 Release rate of <sup>14</sup> C from Zircaloy hulls	3
2.1.2.1 Corrosion rates of Zirconium alloys	3
2.1.2.2 Dissolution rates of zirconia oxide layer	4
2.1.3 Chemical forms of <sup>14</sup> C released	5
2.2 Armines/Subatech contribution in WP3	6
2.2.1 Materials and methods	6
2.2.2 First results	8
2.2.3 Conclusion and perspectives	9
2.3 CEA contribution in WP3	9
2.3.1 Leaching experiments	10
2.3.2 Samples	10
2.3.3 Description of the leaching experiments	13
2.3.4 Analytical strategy	13
2.4 INR contribution in WP3	14
2.4.1 Materials	14
2.4.2 Experimental programme for corrosion and leaching experiments	16
2.4.3 Analytical techniques for the total C-14 measurement	16
2.5 ITU/JRC contribution in WP3	16
2.5.1 Selection and preparation of cladding samples	17
2.5.2 Experimental procedure	17
2.5.2.1 Total C content determination	17
2.5.2.2 Autoclave for leach tests	17
2.5.3 Preparation of the analysis of the leaching aliquots	19
2.6 KIT contribution in WP3	20
2.6.1 Introduction	20
2.6.2 Experimental procedure for quantification of C-14 of irradiated Zircaloy specimens	23
2.6.2.1 Introduction	23
2.6.2.2 Aqueous sample treatment procedure	26
2.6.2.3 Gaseous sample treatment procedure	27
2.7 RWMC contribution in WP3	27
2.7.1 Irradiated Zircaloy cladding (2014)	27
2.7.1.1 Inventory of specimen	27
2.7.1.2 Leaching test	30
2.7.1.3 Chemical form	33
2.7.2 Non-Irradiated Zircaloy cladding	34

2.7.2.1	Confirmation of applicability of high-temperature corrosion equation to low-temperature corrosion	34
2.7.2.2	Influence of key parameters possibly affecting the corrosion rate	39
2.7.3	Acknowledgement	45
2.8	SCK-CEN contribution in WP3	45
2.8.1	Materials	45
2.8.2	Methods and experiments	47
2.8.2.1	Nitrogen analysis	47
2.8.2.2	Corrosion experiments	47
2.8.3	Metallographic analysis	50
2.8.4	Gamma-ray spectrometry analysis	50
2.8.5	Analytical methods for <sup>14</sup> C and carbon analysis	50
3	Summary	52
3.1	Task 3.1 Current status review of Zircaloy and C-14 release	53
3.2	Task 3.2 Development of analytical methods for measuring C-14 speciation	55
3.3	Task 3.3 Characterisation of C-14 released from irradiated zirconium fuel clad wastes	56
4	Conclusion	63
	References	64
	Glossary	67



## 1 Introduction

Work Package 3 (WP3) is related to Zircaloy in the CAST project. It aims to obtain a better understanding of C-14 behaviour in waste Zr fuel claddings under disposal conditions with regard to C-14 inventory (and origins), release from waste packages and speciation of released C-14. In order to achieve these objectives, WP3 has been divided into four tasks (from 3.1 to 3.4) and 20 deliverables (from D3.1 to D3.20).

Task 3.1 is devoted to establishing the State of the Art on the C-14 release from zirconium alloy fuel claddings. Task 3.2 is devoted to developing analytical methods for the characterisation of C-14 organic and inorganic molecules. Task 3.3 is devoted to characterising the C-14 inventory and C-14 release from irradiated zirconium alloy fuel claddings sampled from different BWRs and PWRs. This will be determined from corrosion of activated materials (Zr<sub>2</sub>, Zr<sub>4</sub> and M5) in experiments under conditions relevant to deep geological disposal (cementitious/argillaceous media, aerobic/anaerobic). Acid dissolution of irradiated hulls will be used to measure total amounts of C-14. Finally, Task 3.4 will synthesise the work undertaken in the other tasks in a final report, to develop an interpretation of C-14 behaviour in zirconium alloy fuel claddings (C-14 inventories, release rates and speciation of released C-14) under disposal conditions.

This annual report summarises the work undertaken during the 1<sup>st</sup> year of the CAST Project by all the organisations involved in WP3; Andra, Areva, Armines/Subatech, CEA, INR, ITU, KIT, RWMC and SCK/CEN.

## 2 Progress

This section describes the contributions of the participants in WP3.

### 2.1 *Andra contribution in WP3*

Andra was in charge of the D3.1 in Task 3.1. A literature review was conducted on the State of the Art of C-14 in Zircaloy and Zr alloys – C-14 release from Zirconium alloy hulls.

### 2.1.1 Inventory and distribution of $^{14}\text{C}$ in Zircaloy cladding

In zirconium alloy claddings, the neutron activation of  $^{14}\text{N}$ , impurity element of these alloys, is the main source of  $^{14}\text{C}$  (M.Bordier 2008).  $^{17}\text{O}$  coming from the  $\text{UO}_2$  (or  $(\text{U-Pu})\text{O}_2$ ) oxide fuel and from water coolant is also a significant precursor of  $^{14}\text{C}$  in the zirconia oxide layers formed in reactor on the internal and external sides of cladding respectively. The actual nitrogen content of zirconium alloys is of the order of 30 to 40 ppm (T.Sakuragi, H.Tanabe et al. 2013), that is to say, two times lower than the maximum level of 80 ppm set as specified or contractual values.

Inventories of  $^{14}\text{C}$  in hulls have been determined either by calculation or more rarely by direct measurement (A.Bleier, R.Kroebel et al. 1987; T.Sakuragi, H.Tanabe et al. 2013). For a fuel irradiated at  $\sim 45 \text{ GWd.t}_U^{-1}$ , the production of  $^{14}\text{C}$  in cladding is  $30 \pm 10 \text{ kBq.g}^{-1}$ . The analysis of the collected data shows that the power-related  $^{14}\text{C}$  production amounts to  $1.9 \pm 0.4 \text{ GBq/GWyr.ppm N}$ . Japanese experience (R.Takahashi, M.Sasoh et al. 2013; T.Sakuragi, H.Tanabe et al. 2013; Y.Yamashita, H.Tanabe et al. 2013) suggests that the calculation overestimates the inventory, even when the calculation is carried out with the actual value of the nitrogen content in alloy.

Distribution of  $^{14}\text{C}$  between the metal cladding and the zirconia oxide layer depends on the thickness of the oxide (R.Takahashi, M.Sasoh et al. 2013; T.Sakuragi, H.Tanabe et al. 2013). On PWR fuels irradiated at burn-up  $\geq 45 \text{ GWd.t}_U^{-1}$ , the external oxide layer contains  $\leq 20 \%$  of the  $^{14}\text{C}$  inventory. On BWR fuels, the thinner external oxide layer contains a lower inventory.

There is a lack of reliable data on the chemical state of  $^{14}\text{C}$  in the metal and in the zirconium oxide layer. A modelling approach at the atomic scale would be needed to identify the  $^{14}\text{C}$  insertion sites in the metal and in the oxide.



## 2.1.2 Release rate of $^{14}\text{C}$ from Zircaloy hulls

The mechanisms and the rate of  $^{14}\text{C}$  release from hulls are expected to be controlled largely by the uniform corrosion rate of Zircaloy, the diffusion rate of  $^{14}\text{C}$  from zirconia oxide layers and/or the dissolution rate of zirconia oxide layers, at the time of the contact between hulls and the infiltrated water under the repository conditions. However various questions arise regarding the physical condition of these hulls, i.e., their state of division and fragmentation, at this time. Indeed, the bulk Zircaloy of hulls is hydrided in reactor (D.L.Douglas 1971), linked to the burn-up, which makes the metal brittle and probably more or less fragmented if they are press compacted during waste processing.

### 2.1.2.1 Corrosion rates of Zirconium alloys

Zirconium alloys are highly resistant to uniform corrosion at low or moderate temperatures and their susceptibility to localised corrosion (pitting or crevice corrosion) and stress corrosion cracking appears unlikely in anaerobic groundwaters (M.Pourbaix 1963; C.M.Chen 1983). However, as mentioned above, considerable uncertainties remain regarding the possibility of hydrogen-induced cracking of press compacted hulls under repository conditions. Nevertheless, regardless of the degree of division of hulls, it can be considered that  $^{14}\text{C}$  in the bulk metal of hulls is released congruently with corrosion loss of zirconium alloy. During the corrosion of Zircaloy, there is a possibility of a mechanism in which  $^{14}\text{C}$  is not released immediately by corrosion but is incorporated into the oxide film and then released by diffusion or during the zirconia dissolution. It is supported by the fact that measured  $^{14}\text{C}$  specific concentrations in zirconia oxide layers are about twice of that of Zircaloy metal after irradiation in a reactor.

Various studies (C.M.Hansson 1984; C.M.Hansson 1985; M.Hélie 2004) show that the uniform corrosion rates of zirconium alloys are very low in anaerobic neutral or alkaline waters at low temperature. The envelope value of  $20 \text{ nm.y}^{-1}$ , which has been adopted in some assessment models, seems to be excessively conservative. The most recent results lead to corrosion rates of  $1 \text{ to } 2 \text{ nm.y}^{-1}$  after a few years of a corrosion test. For a corrosion rate of  $1 \text{ nm.y}^{-1}$ , the lifetime of hulls, assuming they are not fractured but are corroded on both



sides, would be of the order of  $2.5 \cdot 10^5$  to  $4 \cdot 10^5$  years, which corresponds to a corroded fraction of  $2.5 \cdot 10^{-6}$  to  $4 \cdot 10^{-6} \text{ y}^{-1}$ . The thickness of metal corroded on each side of hull for 10 half-lives of  $^{14}\text{C}$  would be only of  $\sim 60 \mu\text{m}$ . In other words, such low corrosion rates will lead to decay of much of the inventory of  $^{14}\text{C}$  before release can occur.

However it should be noted that our knowledge on the corrosion resistance of zirconium alloys at low temperature considers the very beginning of the corrosion regime. Study of the corrosion behaviour of Zircaloy in high temperature water has shown that, when the zirconia oxide layer reaches a critical thickness of  $\sim 2.5 \mu\text{m}$  (corresponding to a weight gain of  $30$  to  $40 \text{ mg}\cdot\text{dm}^{-2}$ ), there is a change of the corrosion regime: the corrosion kinetics first follows a power law (*a priori* a cubic law) and after the break-away point corrosion follows pseudo-linear kinetics. It is not possible, at low temperature, to explore the corrosion regime which is beyond a possible phenomenon of break-away, where the corrosion kinetics could be pseudo-linear (IAEA 1998; IAEA 2006). Corrosion tests on pre-oxidized samples (oxide thickness  $> 10 \mu\text{m}$ ) or hulls would complete the range of tests already performed.

The hydrogen pick-up ratio for Zircaloy reaches values of about 90 % in alkaline and in pure water between  $30$  and  $50^\circ\text{C}$  (O.Kato, H.Tanabe et al. 2013). So the non-corroded metal of hulls will be gradually transformed into brittle zirconium hydride, as it corrodes. This will generate on the external surface of hulls a high-density region of hydrides, acting as a brittle layer, and presumably having corrosion behaviour different from that of zirconium metal.

#### 2.1.2.2 Dissolution rates of zirconia oxide layer

The zirconia oxide layer formed on spent fuel rod cladding is chemically very stable in pure water (a solubility of  $10^{-9} \text{ M}$  can be considered as a conservative and realistic estimate). The solubility increases with increasing alkaline concentrations, and reaches values of the order of  $10^{-6} \text{ M}$  at pH 12.5 at ambient temperature (Andra 2005). The zirconia solubility remains very low for carbonate concentrations lower than  $10^{-2} \text{ M}$ . At low to moderate concentrations, chloride ions do not seem to have any significant effect on the zirconia



solubility, except in CaCl<sub>2</sub> solutions of concentration higher than 0.05 M at pH > 10 due to the formation of a highly soluble complex with calcium.

The dissolution rates of zirconia are less well known and have been less studied than the corrosion rates of Zircaloy. In addition, a lack of knowledge of whether the release of radionuclides can be considered as congruent with the dissolution of zirconia has led to the conservative assumption in performance assessment studies that the oxide layer provides no delay to the release of radionuclides. However, in light of some recent results (R.J.Guipponi 2009), a realistic value (but possibly not conservative) of the dissolution rate of zirconia in neutral groundwaters or in cementitious environments that are weakly carbonated (< 0.01 M) and fluoride-free, could be very low (of the order of magnitude: 1 nm.y<sup>-1</sup>).

Recent Japanese leaching experiments (H.Tanabe, T.Nishimura et al. 2007; Y.Yamashita, H.Tanabe et al. 2013) in alkaline solutions at pH 12.5 at room temperature suggest that <sup>14</sup>C release would be congruent with the oxide layer dissolution and metal corrosion.

### 2.1.3 Chemical forms of <sup>14</sup>C released

The aqueous C-H-O system in complete thermodynamic redox equilibrium would be dominated by carbonate and methane. However, complete stable redox equilibrium is seldom achieved in the C-H-O system at moderate temperatures. So the major uncertainties in modelling the C-H-O system are not the uncertainties associated with the thermodynamic data but the model uncertainties, i.e. the question of metastability at moderate temperatures. The chemical stability of organic compounds under the repository conditions is poorly known.

Both organic and inorganic carbons have been identified in leaching experiments (T.Yamaguchi, S.Tanuma et al. 1999; Y.Yamashita, H.Tanabe et al. 2013) with irradiated hulls or non-activated Zr-based materials (Zr and ZrC powders), although a higher proportion is clearly released as small organic molecules. The origin of these compounds and their reaction mechanisms are not fully understood. The finding that small organic molecules such as short-chain carboxylic acids, alcohols and aldehydes are dominant species raises questions regarding the ultimate fate of such molecules. Some significant

uncertainties remain with respect to speciation of  $^{14}\text{C}$  (inorganic vs. organic), as well as the nature of the organic  $^{14}\text{C}$ .

## 2.2 Armines/Subatech contribution in WP3

Armines/Subatech is in charge of analysing the C-14 content in liquid and gas phases. Their contribution is part of Task 3.2 (Development of analytical methods for measuring C-14 speciation) and they are leader of the D3.9 report due in July 2015.

### 2.2.1 Materials and methods

The contribution of Armines/Subatech involves a strong collaboration with CEA who will provide the leaching solution. The definition of the leaching conditions should reflect those existing in storage conditions which could be defined as follows (Figure 1):

- dissolution of alkali hydroxides, pH ~13.5,
- dissolution controlled by the portlandite  $\text{Ca}(\text{OH})_2$  solution, pH ~12.5 (current reference solution in WP3),
- dissolution of hydrated calcium of silicates CSH, pH from 12.5 to 9,
- dissolution of silica.

During the kick-off meeting (25-26 Nov. 2013), WP2 and WP3 reached the conclusion that from an analytical point of view and to represent the long term storage of the wastes, the leaching conditions in portlandite water at pH ~12.5 would be the best compromise.

Moreover, during the WP2&3 meeting (1-2 July 2014) the experimental setups (type of samples, type of solution, duration of experiments....) were discussed. At the end of the meeting, the leaching conditions were confirmed: portlandite  $\text{Ca}(\text{OH})_2$  solution (pH ~12.5).

The experimental procedure suggested is presented in Figure 2. The method is based on the measurement by gamma spectrometry of the leaching solution in contact with irradiated Zircaloy cladding. The measurement will assess the activity level in order to prepare the method to ship the sample from CEA to Armines/Subatech. According to the measurement realised by Yamashita et al. (Y.Yamashita, H.Tanabe et al. 2014), the activity in solution results essentially from  $^{14}\text{C}$ ,  $^{125}\text{Sb}$ ,  $^{60}\text{Co}$  and  $^{137}\text{Cs}$ . The latter is the main contributor of the

activity. The solution containing inorganic and organic carbon will be separated by acidification. The solution containing only organic compounds will be analysed by HPLC and liquid scintillation. The bibliographic research allowed to target the speciation of organic compounds during anaerobic corrosion of Zircaloy cladding, where low chain of carbon (chain with C < 5) would be preferentially released (T.Heikola 2014).

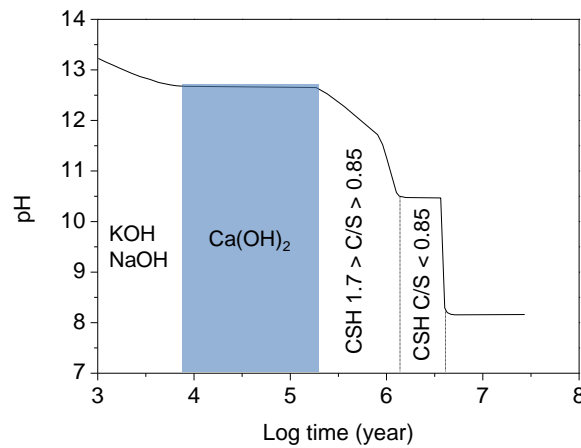


**Figure 1 Evolution of pH as a function of time in the reference case repository (Atkinson, Goult et al. 1985)**

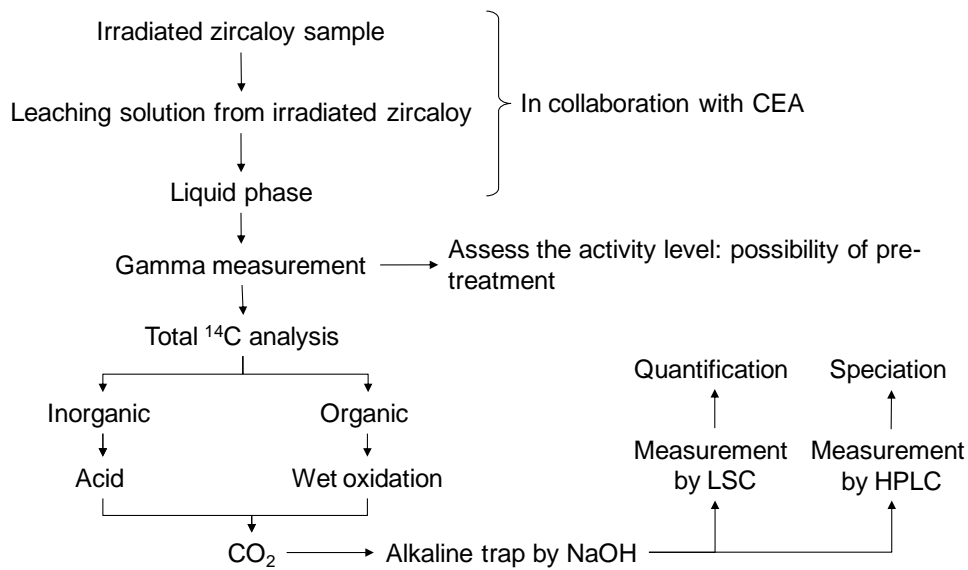


**Figure 2 Experimental setup for Carbon-14 analysis**

## 2.2.2 First results

The experimental procedures have been identified for the separation of the organic carbon compounds. 6 sets of molecules have been selected (acetate, formate, propionate, oxalate, valerate and butyrate) and have been separated with a DIONEX Thermo electron AS11-HC 4 mm-column specifically designed for the separation of inorganic anions and organic acid anions. A gradient (1 – 30 mM in 29 min) of KOH eluent was used to increase the separation of molecules, in particular for formate and propionate which co-elute.

At this stage, the stability of the 6 sets of organic molecules have been prepared in two types of solutions NaOH (pH 12) and Ca(OH)<sub>2</sub> (pH 12.5) to assess the effect of pH or the effect of matrix. All the experiments were prepared in a glove box (Ar gas). The first results are shown in Figure 3. The stability of acetate, formate, propionate and oxalate depends on the concentration and matrix composition:

- Oxalate is the molecule which is not influenced by the concentration and the matrix composition. It exists in all conditions.
- Acetate and formate depend on the concentration but are not influenced by the matrix composition.
- Propionate depends on the concentration and the matrix composition.

Thus, the results indicate that in portlandite solution, oxalate is the most stable molecule and may exist at low concentration. This result is important due to the low concentration expected in the repository (~ppb) and the low dissolution rates of Zircaloy/zirconia (~10 nm/year).

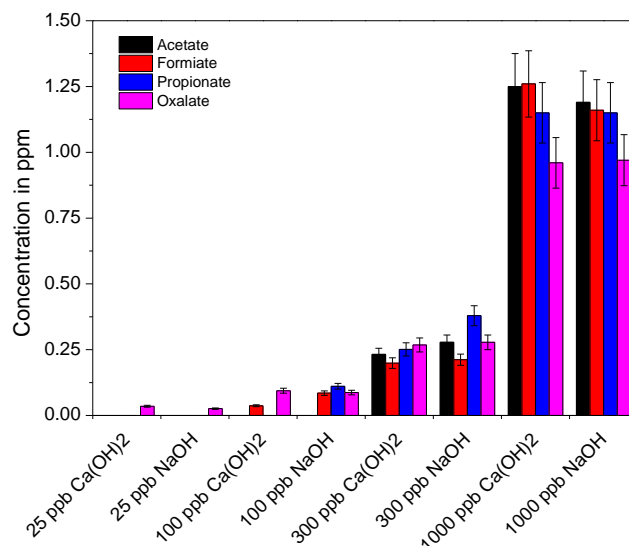


**Figure 3 Evolution of acetate, formate, propionate and oxalate at different concentrations (25, 100, 300 and 1000 ppb) in Ca(OH)<sub>2</sub> and NaOH solutions over 15 days**

Complementary analyses were performed on the stability of these molecules with time. The same set of organic molecules were analysed after 1 min, 6 hours and 24 hours in Ca(OH)<sub>2</sub> solution. The results indicate that only for the case of oxalate, the concentration in solution decreases by a factor 2 indicating a possible precipitation with calcium. The evolution of organic molecules may occur in solution as it has been observed by Yamashita et al. (Y. Yamashita, H. Tanabe et al. 2014) but these results should be confirmed by complementary analyses.

### 2.2.3 Conclusion and perspectives

The methods for the quantification of organic compounds are being investigated.

## 2.3 CEA contribution in WP3

CEA was in charge of the D3.2 in Task 3.3. A report was issued on the definition of operating conditions and presentation of the leaching experiments.

CEA will contribute to the characterisation of the C-14 release from irradiated zirconium alloys in water representative of cement environment. Such characterisations will be carried

out thanks to leaching experiments in shielded cells coupled with chemical analysis of water ( $^{14}\text{C}$  fraction release and  $^{14}\text{C}$  release rate) and metallographic observations.

### 2.3.1 Leaching experiments

Leaching experiments were initially planned at the LECI laboratory in CEA Saclay. Unfortunately, this is now not possible and another laboratory based in CEA Marcoule will take over the leaching experiments in WP3. There might be slight changes in the work programme.

### 2.3.2 Samples

The hulls from PWR reactors are supplied by AREVA. The samples of fuel rods had undergone industrial treatment in AREVA-La Hague reprocessing plant (details are presented in the D3.2 report).

At the beginning of 2014, a selection of hulls held in ATALANTE (Laboratory of dissolution studies, in CEA Marcoule) was chosen. Their characteristics were: cylindrical pieces of claddings with a length of about 35 mm. Leaching experiments and metallographic studies can be carried out among a selection of four types of Zircaloy based alloys (Table 1).

**Table 1 Hulls irradiation characteristics**

Hulls reference	COQ M5	MOX D4	COQ UOX2	COQ UOX3
Cladding material	M5	Inner layer = Zircaloy 4  Outer layer= Zr- 0,8% Sn	Zircaloy 4	Zircaloy 4
Fuel type	UOx  (3,88% <sup>235</sup> U)	MOX  (7,2 % Pu)	UOx  (3,7% <sup>235</sup> U)	UOx  (3,7% <sup>235</sup> U)
Number of cycles	4 cycles	4 cycles	4 cycles	4 cycles
Mean burn-up	46570 MWd/t <sub>HM</sub>	54500 MWd/t <sub>HM</sub>	39700 MWd/t <sub>HM</sub>	48200 MWd/t <sub>HM</sub>
Reactor	EDF PWR 1300 (Nogent 2)	PWR Gösgen (Switzerland)	EDF PWR 900 (Chinon B1)	EDF PWR 900 (Cruas 4)
Discharged from reactor	June 2004	2002	March 1992	1994
Discharged from the hull rinser (La Hague)	October 2009	September 2008	August 1999	June 2004
Arrival in Marcoule (CEA)	2010	2009	1999	July 2004
Number of specimen	4	4	4	4

Currently the samples are held in the LECI laboratory; but they will be shipped soon to the laboratory which is taking over the leaching experiments. The organisation of the samples shipment from ATALANTE to the LECI hot laboratory began in January 2014. Finally, the samples were delivered to the LECI hot laboratory on 28 and 29 July 2014.

Currently, additional information is being looked up on the irradiation characteristics and the initial chemical composition of the claddings; in particular the concentrations of carbon and nitrogen responsible for the presence of C-14.

The selected hulls are shown in Figure 4.

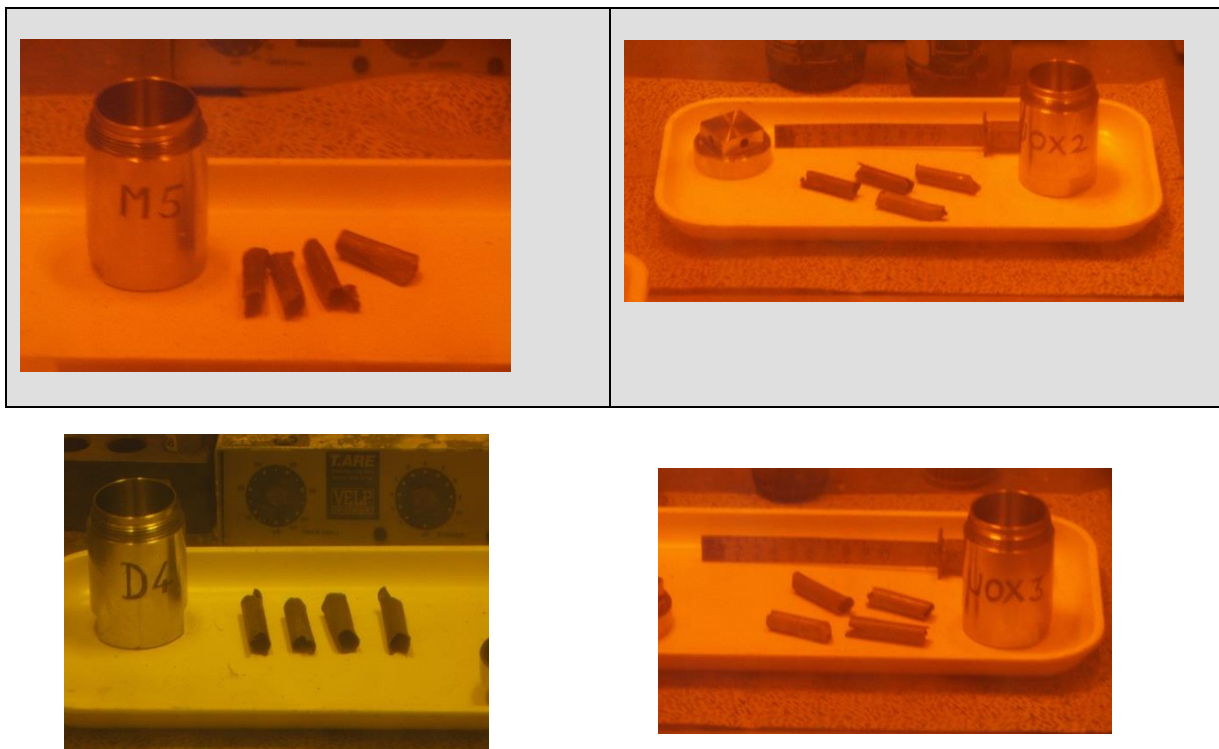


**Figure 4: Photograph (taken through a cell window) of the sheared cladding.**



### 2.3.3 Description of the leaching experiments

Some details about the hot cell and experimental conditions are described in the D3.2 of the CAST project. They concern the work planned by the LECI laboratory and will have to be updated. Leach tests will be conducted in a shielded cell.

Since November 2013, information has been collected from other hot laboratories about protocols of leach tests in a shielded cell, sampling systems and transfer systems to supply the laboratory in charge of C-14 analyses.

### 2.3.4 Analytical strategy

In 2014, an analytical strategy has been established (see Figure 5). The aims of this analytical strategy are to answer to different objectives:

- Information on the size of molecules present in samples;
- Semi-quantitative distribution of the different chemical families (alcohols, ketones, carboxylic acids, etc...);
- Determination of C-14 concentration.

The experimental protocol will be realised as follows:

- 1- Development of a method for quantification of total organic carbon with the aim to determine the carbon mass balance for each leachate solution.
- 2- Development of spectroscopic methods such as infrared-red analysis to identify the main families of chemical functions (carboxylic acids, aromatic compounds, ketones, alcohols, etc...).
- 3- Development of analytical methods based on chromatographic techniques. The aim is the detection and quantification or semi-quantification of targeted families of molecules. For example, ion chromatography will be used for the detection of small carboxylic acids and a coupling between gas chromatography and mass spectrometry will be used for detection of small organic compounds with high polarity.

4- Development of analytical methods based on mass spectrometry (electrospray-mass spectrometry technique) with the aim to detect and identify molecules with high molecular weight.

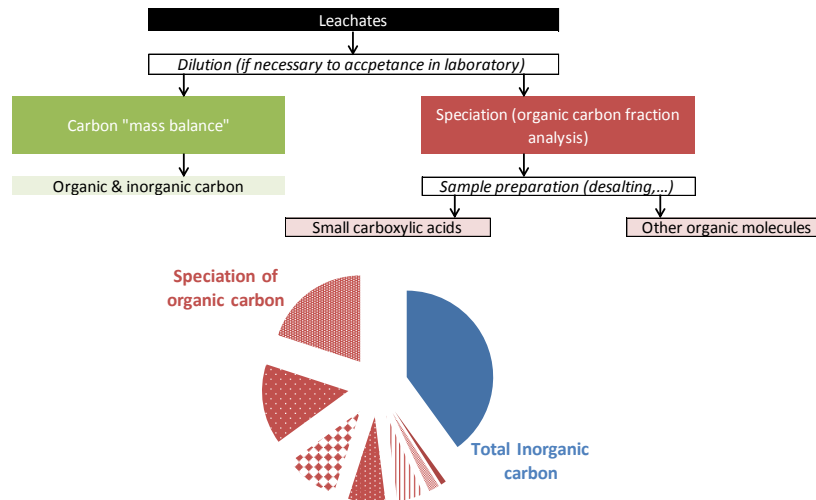


**Figure 5 Presentation of the analytical strategy.**

This analytical strategy has already been demonstrated for the study of the uranium carbide dissolution (S.Legand, C.Bouyer et al. 2014). The analytical approach is the same in both WP3 and WP4.

Applications of analyses by AMS or pre-concentration of solutions for detection of  $^{14}\text{C}$  by LS, will also be developed for very low concentrations.

## 2.4 INR contribution in WP3

### 2.4.1 Materials

INR will work on irradiated Zr-4 samples, which come from a CANDU spent fuel bundle (see Figure 6) transported from Units 1 of Cernavoda NPP to ICN for different investigations. Six irradiated Zr-4 of 15 mm length will be supplied. The protocol for irradiated Zr-4 tube cutting was approved by the ICN managers. In addition, the Cernavoda

NPP agreed to use these samples and publish the experimental results and the irradiation history.



**Figure 6 CANDU fuel bundle**

Each CANDU FA contains around 4.2 kg of Zr-4 (fuel claddings, end-caps, end support plate, inter element spacers and pads). This means that around 1.5E+06 kg of Zr-4 will be disposed of in a geological repository in Romania.

The main design parameters for CANDU spent fuel are summarised in Table 2.

**Table 2 Design parameters for CANDU spent fuel assembly.**

Parameter	Value
FA dimensions:	
diameter (mm)	102
length (mm)	495
Nominal mass (kg)	23.7
U mass (kg)	18.9
Average burn-up (MWday/t U)	7500

## 2.4.2 Experimental programme for corrosion and leaching experiments

Corrosion experiments will be performed both on non-irradiated and irradiated Zr-4 samples (see D3.2 Report). Since corrosion of the irradiated samples is intended to be correlated to the C-14 leaching, the corrosion cell must be adapted in order to be able to use volumes of liquids as small as possible. Therefore, a new 100 ml electrochemical cell, including the electrodes, was ordered to achieve corrosion experiments.

The non-irradiated Zr-4 samples were oxidized in simulated conditions representative of those in the primary circuit.

## 2.4.3 Analytical techniques for the total C-14 measurement

INR will perform analytical measurements to determine the total C-14 content as well as the organic/inorganic carbon fraction (see D3.3 Report).

INR has no previous experience in measuring the organic/inorganic fraction of C-14 from any type of radioactive waste and consequently the components of the experimental set-up for the acid stripping/wet oxidation techniques were purchased. Once all components are assembled, the experimental-set up will be tested using non-radioactive Zr-4 labelled with C-14 standard in order to determine the recovery of the acid stripping/wet oxidation processes. Also the reproducibility and memory effect of the method will be assessed.

## 2.5 ITU/JRC contribution in WP3

ITU/JRC has contributed to the D3.2, D3.3 and D3.4 reports. ITU/JRC is involved in tasks 3.2 and 3.3. The D3.6 and D3.14 reports due in 2015 and 2017 respectively are led by JRC/ITU.



## 2.5.1 Selection and preparation of cladding samples

The test material is standard Zr-4 claddings from a high burn-up (>70 GWd/tU) commercial LWR fuel which is available for the CAST Project.

Samples will be 5 mm rings or half rings of the cladding. They will come from just at or above the fuel line; some samples will be cut from the maximum power position. The latter will be needed to be defuelled mechanically and chemically with nitric acid dissolution. The cutting plans have been prepared and the cutting is due to take place by November 2014. Some metallography of the Zircaloy cladding at maximum power is available. One upper plenum sample will go to metallography, while the other samples will be used for total C content determination. The remainder will go for leach testing in the autoclave. Any excess samples will be retained for future repeat testing.

## 2.5.2 Experimental procedure

### 2.5.2.1 Total C content determination

ITU has located a suitable metallurgical total C determination device adaptable to C-14 determination in the irradiated cladding samples. ITU has discussed the adaptations necessary with the manufacturer for the installation in a hot cell. The technical specifications and justifications have been written and will be sent by November to 3 suppliers. It is anticipated that the purchase will be completed by the end of the year and planning is for 3 months construction and cold commissioning, followed by installation in a hot cell by August/September 2015. First tests could be possible for October 2015, with initial samples in the following months.

### 2.5.2.2 Autoclave for leach tests

ITU already has an unused 150 ml autoclave with a Teflon lining that is available for the cladding testing. An additional heating jacket was purchased in February 2014 for enabling temperatures to go to 250 °C and 150 bar pressure. In fact, the autoclave testing parameters

will be 30 °C and 80 °C and 1-2 bar pressure (the slight pressure can aid the gas sample extraction). The autoclave and the heating mantle are presented in Figure 7. The temperature stability of the heating mantle is currently being tested. Place has been located for the autoclave in a second hot cell. It will need adaptations for detachable connectors to the gas and liquid sampling lines. The corresponding connectors need to be fitted in the hot cell. Ceramic ( $\text{Al}_2\text{O}_3$ ) sample holders also need to be made by the workshops for installation in the autoclave. Introduction of the autoclave should be possible at or just after the year end.



**Figure 7 Autoclave with heating mantle and hot plate for assuring a constant temperature during the leach tests**



### 2.5.3 Preparation of the analysis of the leaching aliquots

A glove box will be required to collect the CO<sub>2</sub> and other gaseous species from the high purity N<sub>2</sub> or Ar gas purge of the autoclave. In addition to the first gas lines to and from the hot cell purging the atmosphere of the autoclave and bringing it to the glove box, a molecular sieve in an ampoule (also additional bottles for H<sup>3</sup> or I removal) will be necessary. The ampoule will then be switched to a second gas line which can purge the CO<sub>2</sub> captured on the sieve and collect it in a liquid with a scintillator ready for counting by using the Liquid Scintillation Counting (LSC) technique. The draft design of the glove box and the necessary chemical glassware and ampoules have been submitted to the workshop. They will be discussed with the drawing office to finalise the construction of the glove box. Items of chemical cleaning equipment (wash-bottles, gas & liquid lines) and analytical chemicals (for LSC absorption & scintillation, active charcoal, certified standards of C-14, high purity Ar & N<sub>2</sub> gas) will also be ordered at the same time.

Aliquots of the liquid phase in the autoclave will be pumped from the autoclave directly into a bottle for transfer from the hot cell to an analytical glove box where the liquid will be acidified and transferred into an alkaline collection bottle with scintillation chemicals so that the liquid aliquot would be ready for scintillation counting. The acquisition of a peristaltic pump will also be undertaken at the end of this year. Certified steel C standards for the total C content determination will also be purchased at this time.

The C-14 analyses will be performed by existing beta (scintillation) counting equipment already performing in house.

For the glove box construction, some cold testing will be necessary before it can be used on actual test aliquots. This can begin as soon as the first 3 months autoclave test starts: this will give sufficient time for practice before the first test sample is ready.

## 2.6 *KIT contribution in WP3*

KIT was in charge of the D3.3 in Task 3.2. A report was issued on the description of the analytical procedure for gaseous and dissolved C-14 species quantification. KIT will lead the D3.8 and D3.15 due in 2015 and 2017 respectively.

### 2.6.1 Introduction

A method that allows the separation and quantification of inorganic and organic/CO C-14 species in gaseous and aqueous samples taken from dissolution experiments with irradiated Zircaloy cladding was developed at KIT-INE. The used Zircaloy cladding is taken from the plenum of a UO<sub>2</sub> fuel rod segment, which was irradiated in the pressurised water reactor at Gösgen, Switzerland (Figure 8). Relevant characteristic parameters of the irradiated material are given in Table 3 and dimensions are given in Figure 9. Small Zircaloy specimens (~100 mg) are used in dissolution experiments, which are conducted in the shielded box line of KIT-INE.



**Table 3 Features of Zircaloy specimen studied by KIT-INE**

<b>Reactor</b>	<b>type: PWR</b> <b>fuel type: UO<sub>2</sub></b> <b>thermal power: 3002 MW</b>
Zircaloy specimen data	material: Zircaloy-4 rod diameter: 10.75 mm wall thickness: 0.725 mm length: 75.3 mm weight: 16.6 g nominal N conc.: 40 ppm (T.Sakuragi, H.Tanabe et al. 2013)
Irradiation data	average burn-up: 50.4 GWd/t <sub>HM</sub> number of cycles: 4 average linear power rate: 260 W/cm maximal linear power rate: 340 W/cm calculated neutron flux: $9.3 \times 10^{13} \text{ cm}^{-2} \text{ s}^{-1}$ date of discharge: 27 May 1989 irradiation duration: 1226 days



**Figure 8 Irradiated Zry-4 plenum specimen used for the dissolution experiments**

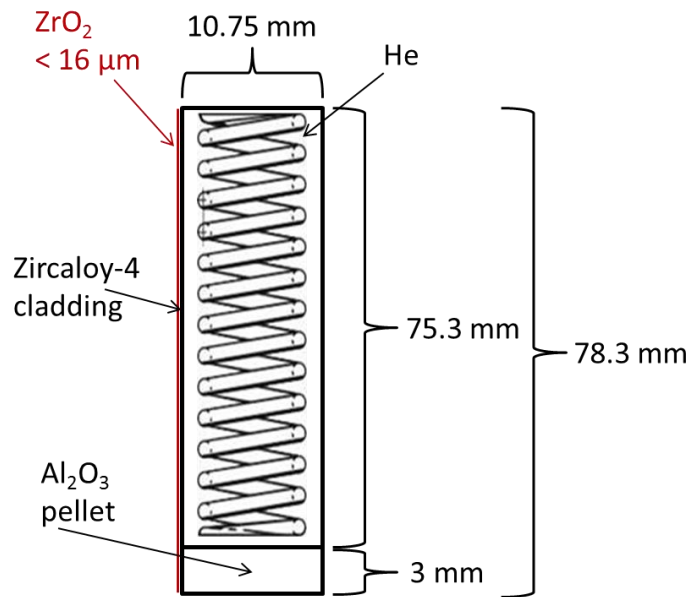


**Figure 9** Scheme of the Zry-4 cladding with the stainless steel plenum spring inside

## 2.6.2 Experimental procedure for quantification of C-14 of irradiated Zircaloy specimens

### 2.6.2.1 Introduction

For determining the inventory/chemical form of C-14, dissolution experiments with specimens of the Zircaloy cladding are going to be performed in autoclaves under reducing conditions at ambient temperature using a dilute HF/H<sub>2</sub>SO<sub>4</sub> mixture. An overview on the experimental programme including extraction and analytical techniques is outlined in Figure 10.

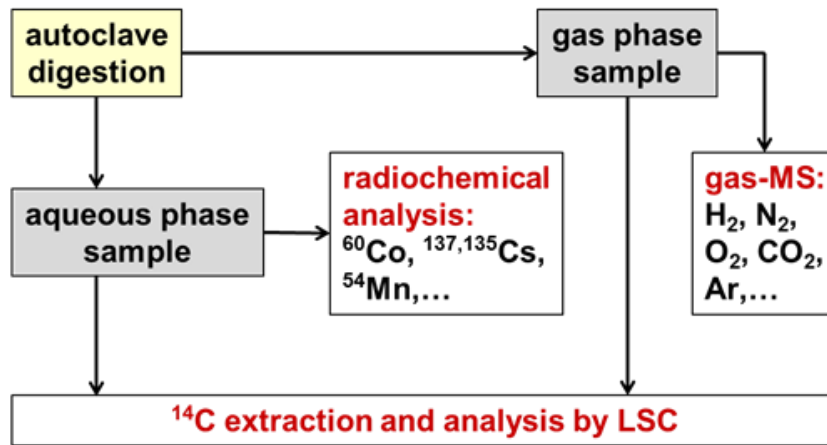
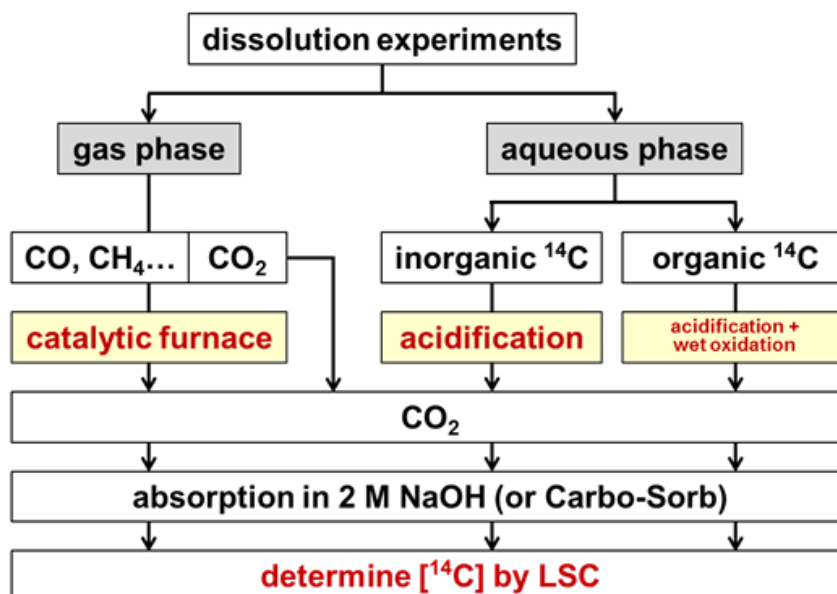


Figure 10 Scheme of the experimental procedure for quantification of C-14 species of Zircaloy specimens.

The analytical C-14 separation procedure, shown in Figure 11 is based on a method developed for determining C-14 in spent ion exchange resins and process water from nuclear reactors (A.Magnusson and K.Stenstroem 2005; A.Magnusson 2007; A.Magnusson, K.Stenstroem et al. 2008). The procedure involves several steps (i.e. acid stripping and wet oxidation) during which the inorganic and organic/CO fractions are extracted and converted into  $\text{CO}_2$  which is then absorbed in washing bottles containing 2 M NaOH. A catalytic furnace between the two sets of washing bottles (first set with bottles #3 and #4, second set with bottles #5 and #6, Figure 12) ensures oxidation of reduced compounds like CO or  $\text{CH}_4$  methane. The content of C-14 in the NaOH solution is finally determined by using the LSC technique.



**Figure 11** Scheme of C-14 extraction procedure for gaseous and dissolved aliquots of experiments with Zircaloy specimens

The experimental design outlined in Figure 12 consists of either a 500 mL three-neck flask with gas-inlet, 120 mL dropping funnel and cooler for aqueous samples or a gas collecting cylinder with two valves for gaseous samples, connected to the CO<sub>2</sub> gas absorption system.

The CO<sub>2</sub> gas absorption system consists of a total of six customised washing bottles filled with 25 mL 2 M NaOH respectively, except bottle #1, which is the I-129 trap and contains 50 mL 0.1 M AgNO<sub>3</sub> and bottle #2, which is the H-3 trap and contains 50 mL 5% H<sub>2</sub>SO<sub>4</sub>. The catalytic furnace consists of a tube furnace operating at 750°C, holding a quartz glass tube which is filled with the catalyst mixture (30 wt.% Pt on Al and 70 wt.% copper oxide wire). The system is interconnected by silicon tubing. Nitrogen, supplied by a gas bottle connected through a buffer volume is used as carrier gas with a flow rate of ~250 mL/min. To prevent the loss of CO<sub>2</sub> gas in the case of a leakage, the system is operated under sub-atmospheric pressure (– 0.2 bar) by means of a diaphragm vacuum pump with fine-adjustment valve and manometer.

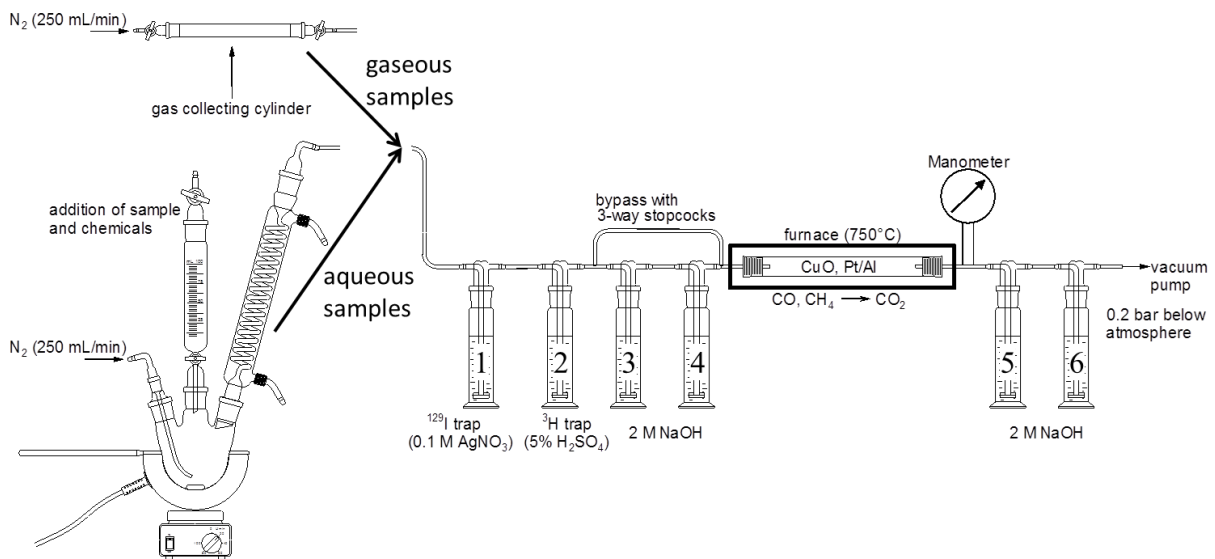


**Figure 12 Experimental design for C-14 extraction of gaseous and dissolved aliquots of experiments with Zircaloy specimens**

### 2.6.2.2 Aqueous sample treatment procedure

Aqueous aliquots, which are sampled from the dissolution experiments, are introduced in the dropping funnel (100 mL) and the system is evacuated at 0.2 bar below atmosphere. Subsequently the nitrogen carrier gas flow rate is set at 250 mL/min. The sample solution is added slowly to the three-neck flask containing a volume of 50 mL 8 M H<sub>2</sub>SO<sub>4</sub>. The solution is purged and stirred for two hours, during which the inorganic fraction is released as CO<sub>2</sub> and absorbed in the washing bottle #3 (Figure 12). Reduced carbon compounds like CO, released during the acid stripping are oxidised in the catalytic furnace and absorbed in washing bottle #5. Prior to the wet oxidation step, washing bottles #3 and #4 are disconnected from the system using the three-way stopcocks. The remaining carbon compounds in the sample solution (organic fraction) are oxidised by a strong oxidant (K<sub>2</sub>S<sub>2</sub>O<sub>8</sub>), catalyst (AgNO<sub>3</sub>), heat and magnetic stirring. Consecutively 50 mL of a 5% potassium peroxodisulfate solution and 5 mL of a 4% AgNO<sub>3</sub> solution are added immediately to the sample container through the dropping funnel under simultaneous heating (~95°C). After one hour the same amounts of potassium peroxodisulfate and silver

nitrate are added to the flask and the mixture is purged, heated and stirred for another hour. After four hours, samples are collected from the washing bottles for LSC measurements.

### 2.6.2.3 Gaseous sample treatment procedure

The gas collecting cylinder with two valves is connected to the first washing bottle of the CO<sub>2</sub> gas absorption system and the nitrogen gas bottle as shown in Figure 12. The pressure in the system is lowered at about 0.2 bar below the atmospheric pressure and the N<sub>2</sub> gas flow rate is set at 250 mL/min. The content of the gas collecting cylinder is flushed into the CO<sub>2</sub> gas absorption system, where carbon dioxide released from inorganic carbon compounds during the dissolution experiments is absorbed in washing bottle #3. Reduced carbon compounds like CO or CH<sub>4</sub> will be oxidised in the catalytic furnace to CO<sub>2</sub> and absorbed in washing bottle #5. After two hours samples will be collected from the washing bottles for LSC measurements.

## 2.7 RWMC contribution in WP3

RWMC has worked on both non-irradiated and irradiated samples and contributed to the D3.1, D3.2, D3.3 and D3.4 reports. RWMC is involved in Tasks 3.1, 3.2 and 3.3. The D3.19 report due in 2017 is led by RWMC.

### 2.7.1 Irradiated Zircaloy cladding (2014)

#### 2.7.1.1 Inventory of specimen

The results of inventory analysis for BWR cladding materials are shown in Table 4. Inventory values are compensated to the values at the time of the start of an immersion test (STEP3; Dec. 2010, STEP1; Mar. 2008) using the half-life of each radionuclides.

**Table 4 Radionuclide inventory of irradiated specimens (BWR)**

Inventory <sup>*1</sup>		C-14	Sb-125	Co-60	Cs-137
Sample		(Bq g <sup>-1</sup> )			
STEP3	Metal	$1.74 \times 10^4$	$1.04 \times 10^7$	$1.17 \times 10^6$	$4.95 \times 10^6$
STEP1	Metal	$2.48 \times 10^4$	$1.24 \times 10^6$	$2.07 \times 10^5$	$1.63 \times 10^6$
	Oxide film <sup>*2</sup>	$5.68 \times 10^4$	$1.71 \times 10^6$	$9.56 \times 10^7$	$4.34 \times 10^5$

\*1. At the start of the leaching test

\*2. Amount of oxide film is converted into the equivalent amount of Zr metal

In the STEP1 result, C-14 concentration of the oxide film was about 2.3 times that of the metal. Sakuragi. (T.Sakuragi 2009) reported that C-14 generated from  $^{17}\text{O}(n, \alpha)^{14}\text{C}$  reaction was almost comparable to C-14 generated from  $^{14}\text{N}(n, \gamma)^{14}\text{C}$  reaction as a result of radioactivation calculation. Since C-14 generated by the radioactivation of O-17 in an oxide film, it is thought that C-14 in an oxide film increased. Sakuragi (T.Sakuragi 2009) indicated that it is important to consider C-14 sorption of the oxide film. Further investigation is required about these influences.

The inventory of C-14 in metal was calculated by three methods described in Table 5, and compared with the measurement result. Comparison was performed by the ratio of the calculated value (C Bq. g<sup>-1</sup>) to the measured value (M Bq g<sup>-1</sup>). The result is shown in Table 5. When the average burnup of a fuel assembly was used, the deviation of C/M was large. By introducing MCNP code to calculate neutron flux at the fuel assembly, C/M is close to 1. Furthermore, it turned out that the amount of C-14 generated can be more precisely evaluated by adding compensation of Sb-125.

**Table 5 Comparison of measured and calculated C-14 inventory in metal**

		Calculation method		
		a	b	c
C/M	STEP3	N.C.	0.94	0.96
	STEP1	1.80	1.08	0.93

Method a: Calculation using ORIGEN code and the average burnup of a fuel assembly

Method b: Calculation using ORIGEN code and MCNP code

Method c: Sb-125 correction

N.C.: not calculated

C-14 distribution among metal and oxide film was calculated from C-14 inventory of the metal and the oxide film which were obtained in Table 5. Thickness of metal part was set up from the optical microscopic observation. Specific weight was calculated as that of Zircaloy and ZrO<sub>2</sub>, respectively. The result is shown in Table 6. Although C-14 concentration in an oxide film was higher than that of metal, almost all C-14 seems to exist in metal. According to Yamaguchi, et.al (T. Yamaguchi 1999), the distribution ratio in the oxide film of PWR cladding is approximately 17%. The reason of the difference is based on the thickness of the oxide film of BWR specimen and PWR specimen tested.

**Table 6 C-14 distribution in metal and oxide film**

	Thickness (μm)	Specific weight (g cm <sup>-3</sup> )	Weight ratio (%)	C-14 inventory (Bq g <sup>-1</sup> )	C-14 distribution (%)
Metal (STEP1)	740.1	6.55	97.8	2.48 × 10 <sup>4</sup>	96.3
Oxide film (STEP1)	19.9	5.49	2.2	4.20 × 10 <sup>4</sup>	3.7

### 2.7.1.2 Leaching test

The results of the leaching tests performed in a solution of NaOH at pH 12.5 degassed with N<sub>2</sub> are shown in Table 7. Total C-14 analysis and inorganic/organic C-14 analysis were carried out for C-14 in liquid phase and Total C-14 analysis was carried out for C-14 in gaseous phase. C-14 remained in the test container was also measured. C-14 was detected in the gaseous phase at 0.5 and 0.75 years. Remaining C-14 in the container could not be detected. In analysis of the liquid phase, the results of the samples immersed for two years showed a wide variation. This tendency will be checked using longer-term test data.

**Table 7 Leaching test results**

Sample No	Hull weight (g)	Test period (years)	Quantity of nuclide leaching (Bq) <sup>4</sup>						C-14 analysis method
			C-14			Sb-125	Co-60	Cs-137	
			Gas	Liquid	Container				
1 STEP 3	5.8763	0.5	1.62 × 10 <sup>-1</sup>	2.06 × 10 <sup>-1</sup>	ND <sup>*2</sup>	3.10 × 10 <sup>1</sup>	2.12 × 10 <sup>0</sup>	1.45 × 10 <sup>2</sup>	Total C-14
				1.34 × 10 <sup>-1</sup> (IC 38%, OC 62%)					IC, OC <sup>*1</sup>
2 STEP 3	5.8060	0.75	1.76 × 10 <sup>-1</sup>	1.91 × 10 <sup>-1</sup>	ND <sup>*2</sup>	2.91 × 10 <sup>1</sup>	1.97 × 10 <sup>1</sup>	6.58 × 10 <sup>1</sup>	Total C-14
				1.57 × 10 <sup>-1</sup> (IC 35%, OC 65%)					IC, OC <sup>*1</sup>
3 STEP 3	5.8415	1.0	ND <sup>*2</sup>	1.40 × 10 <sup>-1</sup>	ND <sup>*2</sup>	5.06 × 10 <sup>1</sup>	1.63 × 10 <sup>1</sup>	7.37 × 10 <sup>2</sup>	Total C-14
				1.28 × 10 <sup>-1</sup> (IC 73%, OC 27%)					IC, OC <sup>*1</sup>
4 STEP 3	5.7924	2.0	ND <sup>*2</sup>	2.49 × 10 <sup>0</sup>	ND <sup>*2</sup>	9.30 × 10 <sup>0</sup>	7.19 × 10 <sup>0</sup>	2.93 × 10 <sup>2</sup>	Total C-14
				3.63 × 10 <sup>0</sup>					
				7.49 × 10 <sup>-1</sup> (IC 18%, OC 82%)					IC, OC <sup>*1</sup>
				6.99 × 10 <sup>-1</sup> (IC 19%, OC 81%)					
5 STEP 3	5.8457	3.0	6.54 × 10 <sup>-2</sup>	1.26 × 10 <sup>0</sup>	ND <sup>*3</sup>	4.51 × 10 <sup>1</sup>	1.42 × 10 <sup>2</sup>	5.04 × 10 <sup>2</sup>	Total C-14
				1.02 × 10 <sup>0</sup> (IC 30%, OC 70%)					IC, OC <sup>*1</sup>
6 STEP 1	7.7466	5.5	5.11 × 10 <sup>-2</sup>	1.61 × 10 <sup>0</sup>	ND <sup>*3</sup>	1.98 × 10 <sup>1</sup>	3.94 × 10 <sup>1</sup>	1.25 × 10 <sup>3</sup>	Total C-14
				1.07 × 10 <sup>0</sup> (IC 31%, OC 69%)					IC, OC <sup>*1</sup>

\*1. IC: Inorganic carbon; OC: Organic carbon; \*2. ND: not detectable

\*3. C-14 could not be identified and quantified in the H-3 beta-ray spectrum.

\*4 Decrement of radioactivity value of each radionuclide leached are corrected to the value at the start of the immersion test by using the half-life of each radionuclide.

The test results were compared with the results obtained with a Zry-4 cladding from PWR (Figure 13) (T. Yamaguchi 1999). Up to one-year immersion, the BWR samples showed a lower C-14 release fraction than that of the PWR samples. The reason for the different release fraction between the PWR cladding and the BWR cladding might be based on the different effect of hydride and neutron irradiation in a reactor.

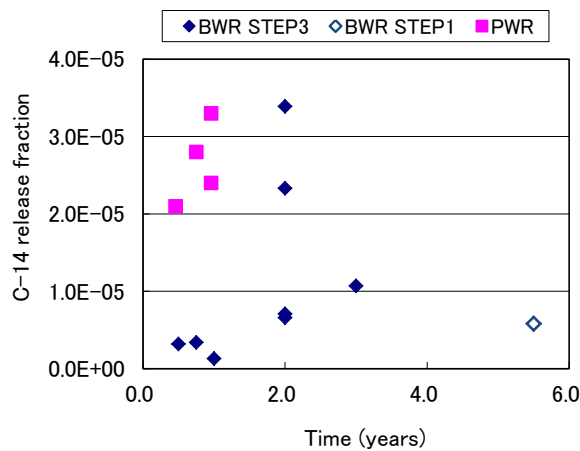


**Figure 13 Comparison between BWR and PWR claddings**

Figure 14 shows a comparison with the results of a corrosion test using unirradiated Zry metal (O.Kato 2013).

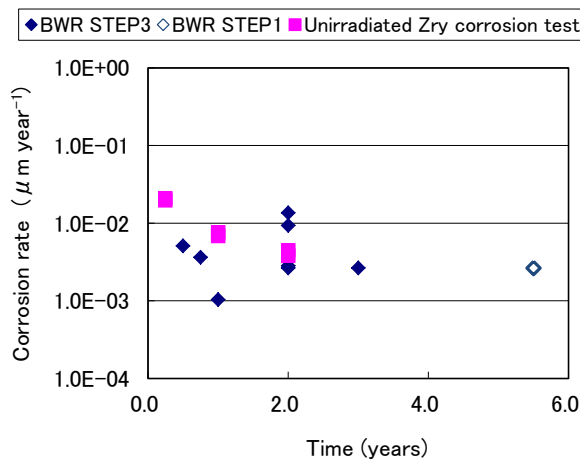


**Figure 14 Comparison between BWR cladding and unirradiated Zry**

The BWR samples showed a lower corrosion rate than the unirradiated Zry samples. The largest difference between these samples was whether or not they had been subjected to neutron irradiation. Neutron irradiation has various effects on the corrosion resistance of materials (Y.Etoh, S.Shimada et al. 1992; IAEA 1998; Hagi 2005), including both improvement and deterioration of corrosion resistance, and it is thought that the corrosion resistance was greatly improved by neutron irradiation in our tests. According to Etoh (Y.Etoh, S.Shimada et al. 1992), the nodular corrosion resistance of Zry is improved with a small dose of fast neutrons because precipitates that exist in Zry, such as Fe, Cr, and Ni, are dissolved into the Zr grains by neutron irradiation. However, the C-14 release rates of the samples immersed for two years showed a large variation, and the average value was almost equivalent to the results of the non-irradiated Zry corrosion test. To explain this behaviour, further investigation based on longer-term test results will be needed.

Figure 15 shows a comparison of the release fractions of C-14 and gamma-emitting radionuclides.

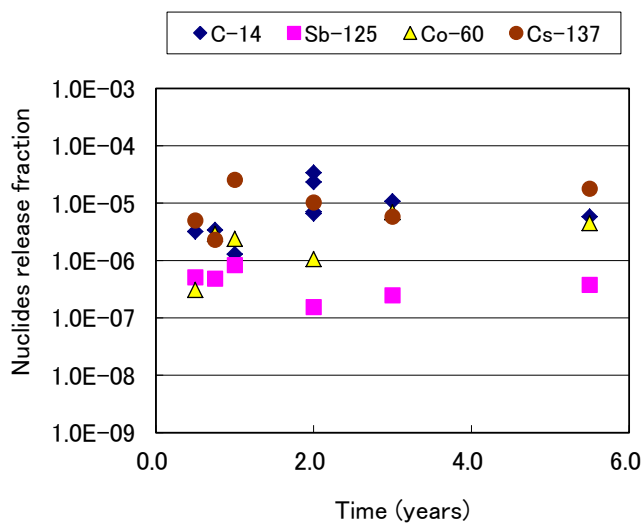


**Figure 15 Comparison with gamma nuclides**

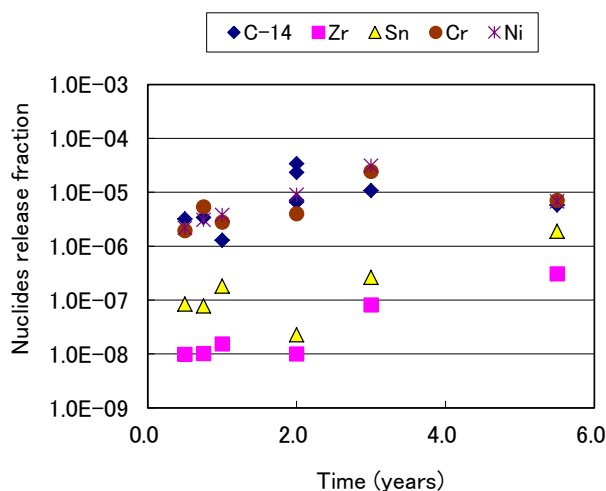


**Figure 16 Comparison with non-radioactive elements**

When compared with the gamma nuclides, after one year, the C-14 release rate was comparable to those of Sb-125 and Co-60, which are activated products, but at two years, the C-14 release rate was comparable to that of Cs-137, which is a fission product. It seems that Cs-137 is not directly related with the release of C-14 because Cs-137 is produced by nuclear fission and injected into claddings as a recoil atom at the time of sample pre-treatment. It will be necessary to examine this in more detail in future work. Figure 16 shows a comparison of the release fractions of C-14 and non-radioactive elements. Compared with C-14, the release fractions of Zr and Sn, which are basic components of Zry, were small, whereas those of Ni and Cr were comparable. The C-14 release behaviour may be related to the forms in which these elements exist in the oxide film.

### 2.7.1.3 Chemical form

Figure 17 shows the C-14 chemical form analysis results of the gaseous phase and the liquid phase. Although 50% of C-14 existed in the gaseous phase until 9 months, it was not detected after 9 months. In the liquid phase, both organic and inorganic C-14 co-existed, and the amount of organic C-14 was higher than that of inorganic C-14, except in the samples immersed for 1 year.

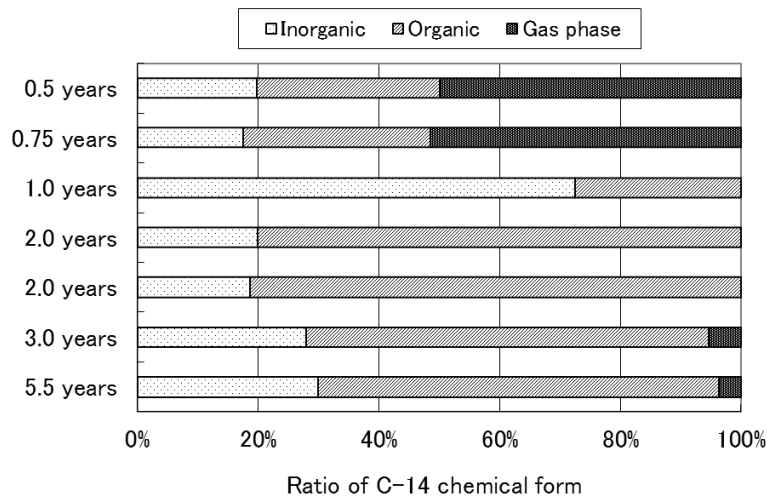


**Figure 17 Chemical form**

Yamaguchi (T. Yamaguchi 1999) reported that C-14 released from a PWR sample was detected only in the liquid phase and most of the C-14 was in the organic form. For both the BWR and PWR claddings, the release rate of organic C-14 was higher than that of inorganic C-14.

## 2.7.2 Non-Irradiated Zircaloy cladding

### 2.7.2.1 Confirmation of applicability of high-temperature corrosion equation to low-temperature corrosion

#### 2.7.2.1.1 Zry corrosion rate in pure water and changes over time at lower temperature ranges

The equivalent corrosion rates calculated by released and absorbed hydrogen in pure water are given in Figure 18. The equivalent corrosion rate for Zry-4 in pure water at 180 days immersion was  $8 \times 10^{-3} \mu\text{m/y}$  at 303 K. Equivalent corrosion rates increased with an increase in temperature from 303 K to 353 K.

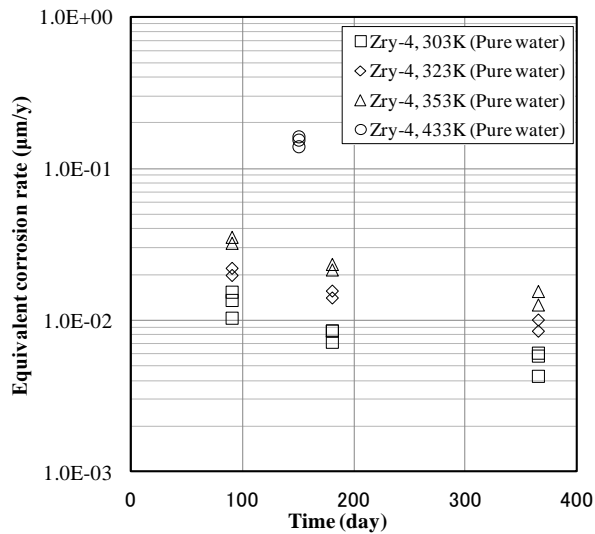


**Figure 18** Equivalent corrosion rates with Zry-4 in pure water

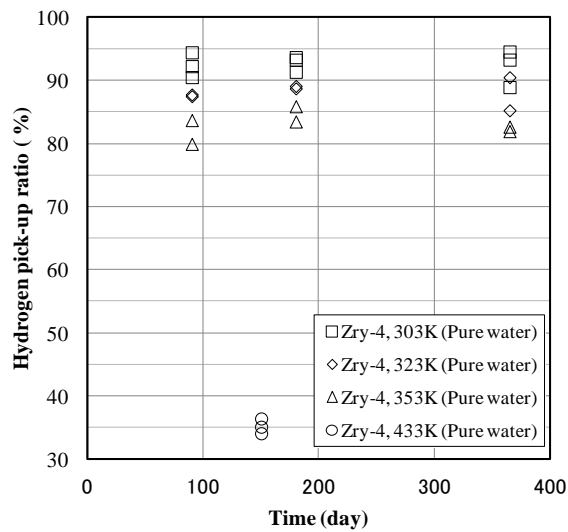


**Figure 19** Hydrogen pick-up ratio with Zry-4 in pure water

The hydrogen pick-up ratio of Zry-4 is shown in Figure 19. The pick-up ratio was about 80–95% and decreased with an increase in temperature from 303 K to 353 K. The pick-up ratio was about 35% at 433 K.

It has previously been established for high-temperature corrosion that the Zry corrosion rate in the pre-transition region (IAEA 1998) obeys the square rate law ( $\Delta W = k \times t^{1/2}$ ) in the initial period of the high-temperature test and gradually shifts to the cubic rate law ( $\Delta W = k \times t^{1/3}$ ), where  $\Delta W$  is the weight gain,  $k$  is the rate constant, and  $t$  is time (Hagi 2005). To

evaluate time-dependent changes, data fitting was performed for the data at 303 K and 353 K in alkaline water using the power law ( $\Delta W = a \times t^b$ ), and multiplier changes were checked for the test period.

The equivalent corrosion rate during the initial period of the low-temperature test was higher than the approximation line of the cubic rate law ( $\Delta W = k \times t^{1/3}$ ), and the data was close to the approximation line of the square rate law ( $\Delta W = k \times t^{1/2}$ ). The data then appears to gradually approach the line of the cubic rate law (Figure 20).

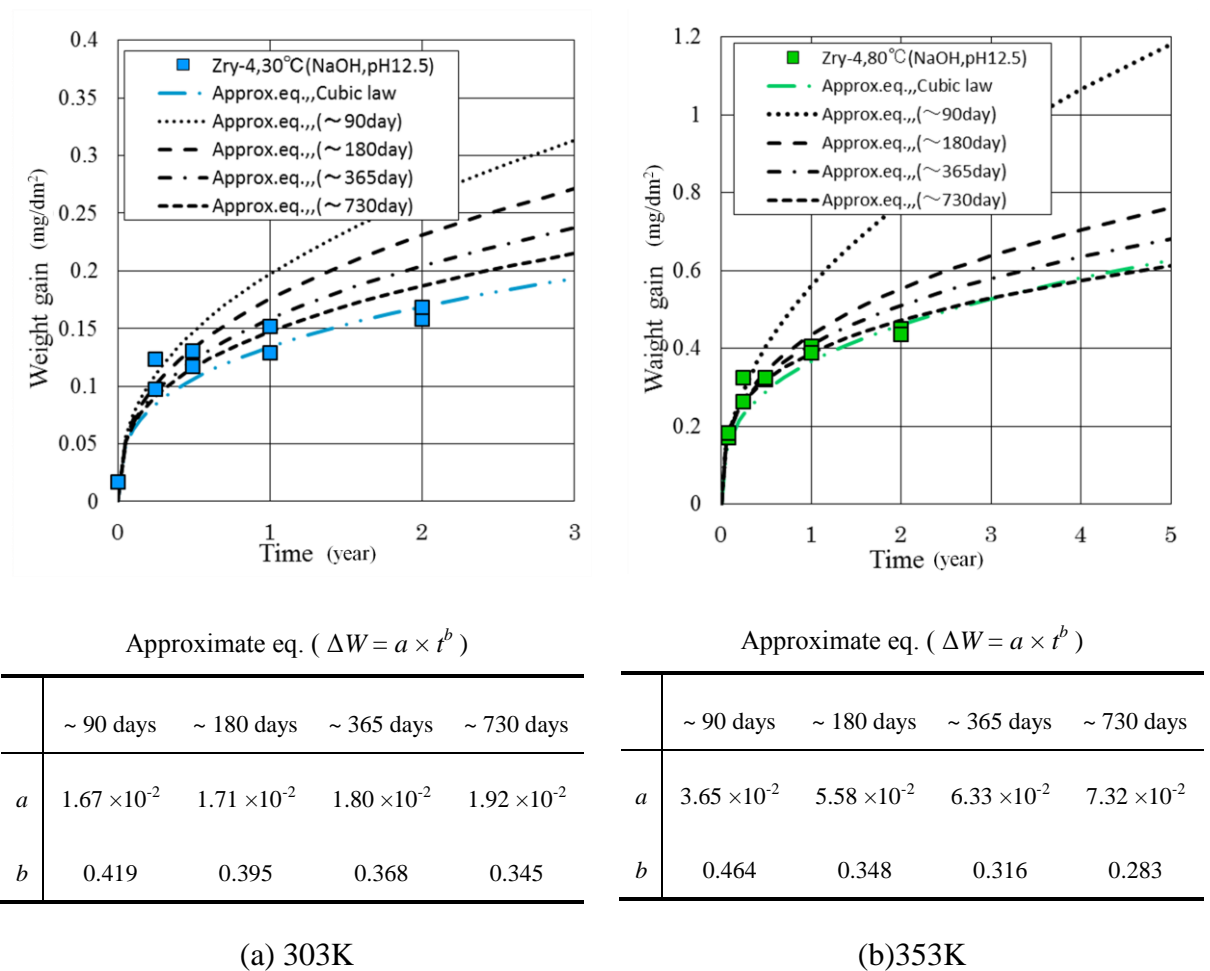


**Figure 20** Fitting results of a low temperature corrosion test result

**2.7.2.1.2 Influence of corrosion rate measurement method**

To evaluate the influence of the measurement method, weight gain was measured at 433 K with the amount of hydrogen using the hydrogen measurement method. The equivalent

corrosion rate evaluated from weight gain measurement techniques were  $1.3 \times 10^{-1}$ ,  $1.5 \times 10^{-1}$ , and  $1.4 \times 10^{-1} \mu\text{m}/\text{y}$  (Table 8). The equivalent corrosion rate evaluated from weight gain measurement and the hydrogen measurement method were in agreement within a 10% range of error.

**Table 8 Comparison of equivalent corrosion rates in measurement method (hydrogen measurement and weight gain)**

Test No.	Material	Solution	Temp. (K)	Period (months)	Amount of hydrogen generation ( $\text{mol} \cdot \text{dm}^{-2}$ )	Weight (g)		Weight gain ( $\text{mg} \cdot \text{dm}^{-2}$ )	Equivalent corrosion rate ( $\mu\text{m} \cdot \text{y}^{-1}$ )	
						Before test	After test		Hydrogen measurement	Weight gain
						1-7-1	Zry-4	Pure water		
1-7-2	Zry-4	Pure water	433	5	$1.9 \times 10^{-2}$	3.56844	3.57012	1.40	$1.6 \times 10^{-1}$	$1.5 \times 10^{-1}$
1-7-3	Zry-4	Pure water	433	5	$1.8 \times 10^{-2}$	3.60780	3.60938	1.32	$1.6 \times 10^{-1}$	$1.4 \times 10^{-1}$

#### 2.7.2.1.3 Influence of annealing condition differences in actual Zry tube and test specimen

In this test, the specimen was annealed at 1023 K. The accumulated annealing parameter,  $\Sigma A_i$  (Garzarolli 1989), of the specimen was found to be  $10^{-16}$ . This parameter is approximately 10 times larger than that of the actual Zry tube product used in high temperature tests.

F. Garzarolli (Garzarolli 1989) showed that there is no significant difference in corrosion resistance in the range of  $\Sigma A_i = 10^{-17} - 10^{-16}$ . Thus, it was assumed that there is no significant difference in the corrosion resistance of the specimen in this test and the actual Zry tube. The particle diameter of intermetallic precipitates increased with  $\Sigma A_i$  increases and affected Zry corrosion rates.

The particle diameter of the intermetallic precipitates in the specimen used for this corrosion test was identified by SEM (Figure 21). The mean particle diameter of the intermetallic precipitates was  $0.25 \mu\text{m}$ . F. Garzarolli showed that the mean particle diameter was

0.18–0.32  $\mu\text{m}$  at  $\Sigma A_i = 10^{-16}$ . The results for this test specimen were in agreement with this finding.

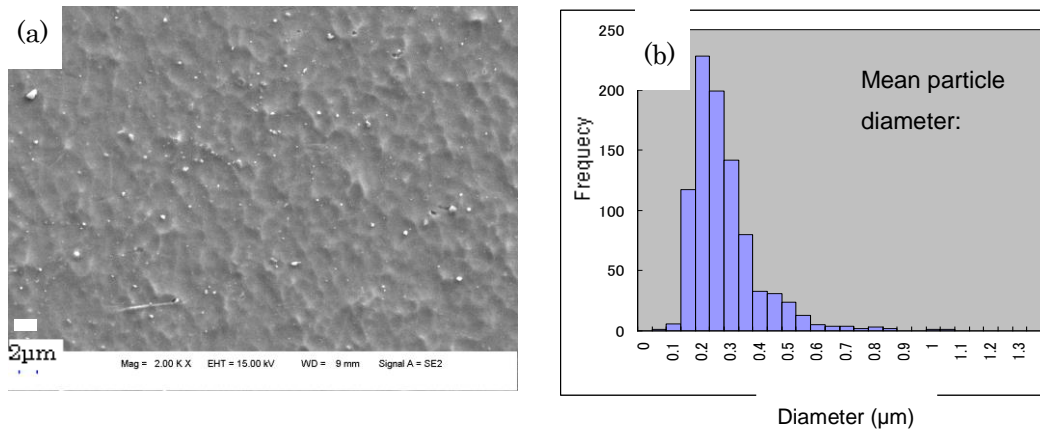


**Figure 21 SEM images and particle diameter of Zircaloy-4 intermetallic precipitates**  
**(a) SEM images, (b) Distribution of particle diameters**

#### 2.7.2.1.4 Influence of composition differences in actual Zry tube and test specimen

The composition of the actual Zry tube differs slightly from that of the corrosion test specimen, in that the Sn concentration in the older Zry tube is slightly greater. But no significant differences in the corrosion rate at 593–633 K were observed (K. Takeda 1996); thus, it was assumed that the influence of this difference on the corrosion rate at low temperatures was not significant as well.

#### 2.7.2.1.5 Property of the oxide film forming at low temperatures

The thicknesses of the oxide films were about 15 nm (323 K, 1825 days, pH 12.5) and 20 nm (353 K, 730 days, pH 12.5) in TEM analysis. Oxygen atoms were observed in EDX analysis and crystallization was observed in electron diffraction analysis. The crystal structure was determined to be orthorhombic or tetragonal, and the monoclinic system observed in high-temperature tests (IAEA 1998) was not observed in either specimens. The equivalent corrosion rates measured with the hydrogen measurement technique were  $7.5 \times 10^{-3} \mu\text{m}/\text{y}$  (323 K, 1825 days, pH 12.5) and  $1.0 \times 10^{-2} \mu\text{m}/\text{y}$  (353 K, 730 days, pH 12.5). The

thicknesses of the oxide films calculated from the equivalent corrosion rate were approximately 15 nm and 20 nm respectively, based on an assumed  $ZrO_2$  density of  $5.5 \text{ g/cm}^3$ .

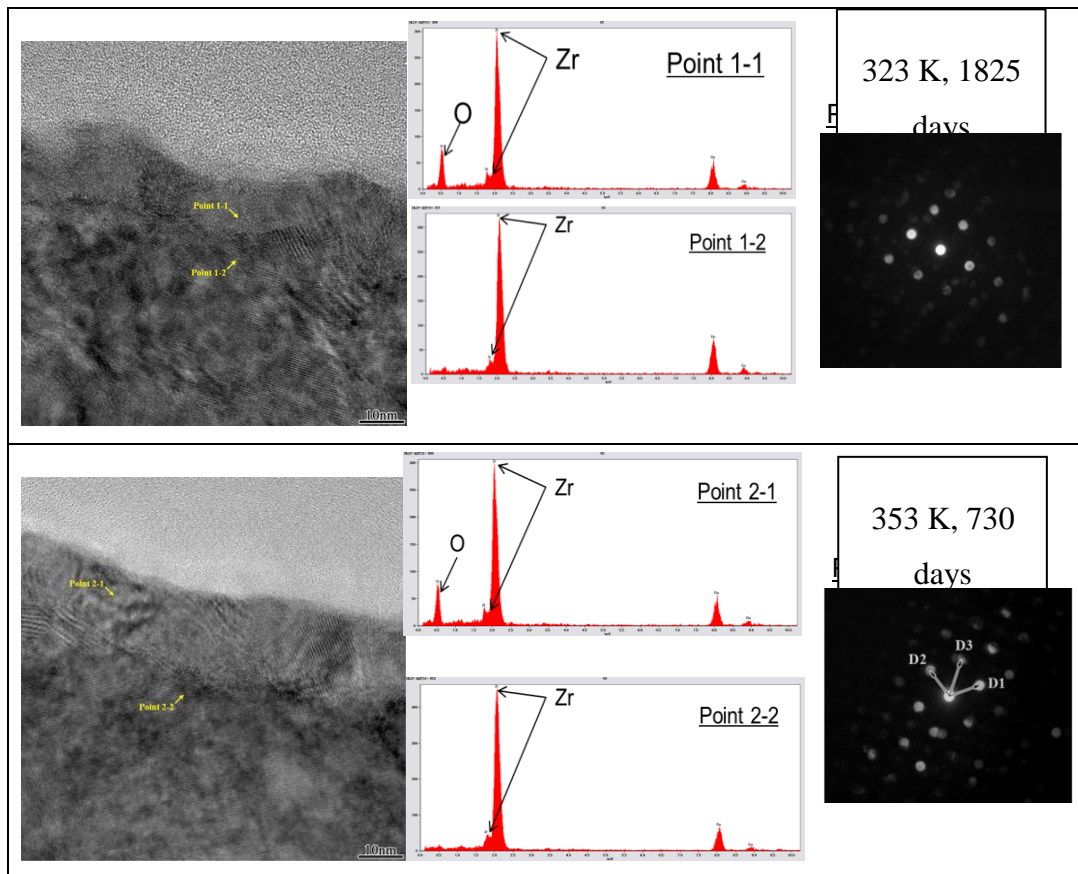


Figure 22 TEM-EDX and electron diffraction for Experiments 2-10-1 (323 K, 1825 days, pH 12.5) and 2-15-1 (353 K, 730 days, pH 12.5)

### 2.7.2.2 Influence of key parameters possibly affecting the corrosion rate

#### 2.7.2.2.1 Material factor (Zircaloy type)

The equivalent corrosion rates and hydrogen pick-up ratios with Zry-4 and Zry-2 in alkaline water (pH 12.5) are shown in Table 9. The equivalent corrosion rate of Zry-4 was within approximately 15% agreement with that of Zry-2. The difference between the two equivalent corrosion rates over the 730 days of immersion was not significant.



**Table 9 Corrosion test results**

Test No.	Material	Solution	pH	Temp. (K)	Period (days)	Amount of hydrogen (H-mol·m <sup>-2</sup> )		Hydrogen pick-up ratio (%)	Equivalent corrosion rate (µm·y <sup>-1</sup> )	Equivalent weight gain (mg·dm <sup>-2</sup> )		
						Released	Absorbed					
						(a)	(b)	(b)/[(a)+(b)]				
1-1-1	Zry-4	Pure water	*	303	90	6.8×10 <sup>-5</sup>	6.5×10 <sup>-4</sup>	90.5	1.0×10 <sup>-2</sup>	5.6×10 <sup>-2</sup>		
1-1-2						8.2×10 <sup>-5</sup>	9.9×10 <sup>-4</sup>	92.2	1.5×10 <sup>-2</sup>	8.4×10 <sup>-2</sup>		
1-1-3			5.2×10 <sup>-5</sup>	8.9×10 <sup>-4</sup>	94.4	1.4×10 <sup>-2</sup>	7.8×10 <sup>-2</sup>					
1-2-1			7.4×10 <sup>-5</sup>	1.1×10 <sup>-3</sup>	93.7	8.5×10 <sup>-3</sup>	9.5×10 <sup>-2</sup>					
1-2-2			8.6×10 <sup>-5</sup>	9.1×10 <sup>-4</sup>	91.3	7.2×10 <sup>-3</sup>	8.0×10 <sup>-2</sup>					
1-2-3			7.9×10 <sup>-5</sup>	1.1×10 <sup>-3</sup>	93.3	8.5×10 <sup>-3</sup>	9.5×10 <sup>-2</sup>					
1-3-1			1.3×10 <sup>-4</sup>	1.1×10 <sup>-3</sup>	89.9	4.3×10 <sup>-3</sup>	9.4×10 <sup>-2</sup>					
1-3-2			8.8×10 <sup>-5</sup>	1.6×10 <sup>-3</sup>	94.6	5.8×10 <sup>-3</sup>	1.3×10 <sup>-1</sup>					
1-3-3			1.1×10 <sup>-4</sup>	1.6×10 <sup>-3</sup>	93.3	6.1×10 <sup>-3</sup>	1.3×10 <sup>-1</sup>					
1-4-1			1.9×10 <sup>-4</sup>	1.3×10 <sup>-3</sup>	87.4	2.2×10 <sup>-2</sup>	1.2×10 <sup>-1</sup>					
1-4-2			1.7×10 <sup>-4</sup>	1.2×10 <sup>-3</sup>	87.7	2.0×10 <sup>-2</sup>	1.1×10 <sup>-1</sup>					
1-5-1			2.2×10 <sup>-4</sup>	1.7×10 <sup>-3</sup>	88.7	1.4×10 <sup>-2</sup>	1.6×10 <sup>-1</sup>					
1-5-2			2.4×10 <sup>-4</sup>	1.9×10 <sup>-3</sup>	89.1	1.6×10 <sup>-2</sup>	1.8×10 <sup>-1</sup>					
1-6-1			2.7×10 <sup>-4</sup>	2.6×10 <sup>-3</sup>	90.5	1.0×10 <sup>-2</sup>	2.2×10 <sup>-1</sup>					
1-6-2			3.5×10 <sup>-4</sup>	2.0×10 <sup>-3</sup>	85.2	8.5×10 <sup>-3</sup>	1.9×10 <sup>-1</sup>					
1-7-1			4.5×10 <sup>-4</sup>	1.8×10 <sup>-3</sup>	79.8	3.2×10 <sup>-2</sup>	1.8×10 <sup>-1</sup>					
1-7-2			4.0×10 <sup>-4</sup>	2.1×10 <sup>-3</sup>	83.6	3.5×10 <sup>-2</sup>	2.0×10 <sup>-1</sup>					
1-8-1			4.9×10 <sup>-4</sup>	2.5×10 <sup>-3</sup>	83.4	2.2×10 <sup>-2</sup>	2.5×10 <sup>-1</sup>					
1-8-2			4.6×10 <sup>-4</sup>	2.8×10 <sup>-3</sup>	85.8	2.3×10 <sup>-2</sup>	2.6×10 <sup>-1</sup>					
1-9-1			7.9×10 <sup>-4</sup>	3.6×10 <sup>-3</sup>	81.8	1.6×10 <sup>-2</sup>	3.4×10 <sup>-1</sup>					
1-9-2	6.2×10 <sup>-4</sup>	3.0×10 <sup>-3</sup>	82.6	1.3×10 <sup>-2</sup>	2.8×10 <sup>-1</sup>							
1-10-1	1.1×10 <sup>-2</sup>	5.5×10 <sup>-3</sup>	33.9	1.4×10 <sup>-1</sup>	1.3							
1-10-2	1.2×10 <sup>-2</sup>	6.6×10 <sup>-3</sup>	34.9	1.6×10 <sup>-1</sup>	1.5							
1-10-3	1.1×10 <sup>-2</sup>	6.5×10 <sup>-3</sup>	36.2	1.6×10 <sup>-1</sup>	1.5							
2-1	Zry-4	NaOH	12.5	303	90	9.2×10 <sup>-5</sup>	1.1×10 <sup>-3</sup>	92.3	1.7×10 <sup>-2</sup>	9.5×10 <sup>-2</sup>		
2-2-1			12.5	303	180	1.1×10 <sup>-4</sup>	1.5×10 <sup>-3</sup>	93.5	1.2×10 <sup>-2</sup>	1.3×10 <sup>-1</sup>		
2-2-2			12.5	303	365	1.2×10 <sup>-4</sup>	1.3×10 <sup>-3</sup>	91.7	1.1×10 <sup>-2</sup>	1.2×10 <sup>-1</sup>		
2-3-1			12.5	303	365	1.5×10 <sup>-4</sup>	1.7×10 <sup>-3</sup>	91.9	6.7×10 <sup>-3</sup>	1.5×10 <sup>-1</sup>		
2-3-2			12.5	303	365	1.3×10 <sup>-4</sup>	1.5×10 <sup>-3</sup>	92.1	5.7×10 <sup>-3</sup>	1.3×10 <sup>-1</sup>		
2-4-1			12.5	303	730	2.0×10 <sup>-4</sup>	1.8×10 <sup>-3</sup>	90.1	3.5×10 <sup>-3</sup>	1.6×10 <sup>-1</sup>		
2-4-2			12.5	303	730	1.7×10 <sup>-4</sup>	1.9×10 <sup>-3</sup>	92.1	3.7×10 <sup>-3</sup>	1.7×10 <sup>-1</sup>		
2-5-1			12.5	323	30	1.8×10 <sup>-4</sup>	1.0×10 <sup>-3</sup>	84.7	5.2×10 <sup>-2</sup>	9.7×10 <sup>-2</sup>		
2-5-2			12.5	323	90	2.0×10 <sup>-4</sup>	9.9×10 <sup>-4</sup>	83.2	5.1×10 <sup>-2</sup>	9.5×10 <sup>-2</sup>		
2-6			12.5	323	90	2.9×10 <sup>-4</sup>	1.7×10 <sup>-3</sup>	87.1	2.9×10 <sup>-2</sup>	1.6×10 <sup>-1</sup>		
2-7-1			12.5	323	180	2.5×10 <sup>-4</sup>	2.3×10 <sup>-3</sup>	88.4	1.8×10 <sup>-2</sup>	2.0×10 <sup>-1</sup>		
2-7-2			12.5	323	180	3.0×10 <sup>-4</sup>	2.0×10 <sup>-3</sup>	87.9	1.6×10 <sup>-2</sup>	1.8×10 <sup>-1</sup>		
2-8-1			12.5	323	365	2.7×10 <sup>-4</sup>	2.7×10 <sup>-3</sup>	87.7	1.1×10 <sup>-2</sup>	2.5×10 <sup>-1</sup>		
2-8-2			12.5	323	365	3.8×10 <sup>-4</sup>	2.1×10 <sup>-3</sup>	86.3	8.4×10 <sup>-3</sup>	1.9×10 <sup>-1</sup>		
2-9-1			12.5	323	730	3.2×10 <sup>-4</sup>	2.6×10 <sup>-3</sup>	85.4	5.4×10 <sup>-3</sup>	2.4×10 <sup>-1</sup>		
2-9-2			12.5	323	730	4.4×10 <sup>-4</sup>	3.1×10 <sup>-3</sup>	88.8	6.2×10 <sup>-3</sup>	2.8×10 <sup>-1</sup>		
2-10-1			12.5	323	1825	3.8×10 <sup>-4</sup>	4.1×10 <sup>-3</sup>	88.3	3.3×10 <sup>-3</sup>	3.7×10 <sup>-1</sup>		
2-10-2			12.5	323	1825	5.4×10 <sup>-4</sup>	3.5×10 <sup>-3</sup>	85.1	2.9×10 <sup>-3</sup>	3.3×10 <sup>-1</sup>		
2-11-1			12.5	353	30	4.8×10 <sup>-4</sup>	1.6×10 <sup>-3</sup>	77.1	9.2×10 <sup>-2</sup>	1.7×10 <sup>-1</sup>		
2-11-2			12.5	353	30	5.3×10 <sup>-4</sup>	1.7×10 <sup>-3</sup>	76.2	9.8×10 <sup>-2</sup>	1.8×10 <sup>-1</sup>		
2-12			12.5	353	90	7.0×10 <sup>-4</sup>	2.7×10 <sup>-3</sup>	82.5	4.7×10 <sup>-2</sup>	2.6×10 <sup>-1</sup>		
2-13-1			12.5	353	180	5.7×10 <sup>-4</sup>	3.3×10 <sup>-3</sup>	81.8	2.8×10 <sup>-2</sup>	3.1×10 <sup>-1</sup>		
2-13-2			12.5	353	180	7.2×10 <sup>-4</sup>	3.5×10 <sup>-3</sup>	85.2	2.9×10 <sup>-2</sup>	3.2×10 <sup>-1</sup>		
2-14-1			12.5	353	365	5.9×10 <sup>-4</sup>	4.3×10 <sup>-3</sup>	85.2	1.8×10 <sup>-2</sup>	4.1×10 <sup>-1</sup>		
2-14-2			12.5	353	365	7.4×10 <sup>-4</sup>	4.0×10 <sup>-3</sup>	82.4	1.7×10 <sup>-2</sup>	3.8×10 <sup>-1</sup>		
2-15-1			12.5	353	730	8.4×10 <sup>-4</sup>	4.7×10 <sup>-3</sup>	84.2	1.0×10 <sup>-2</sup>	4.5×10 <sup>-1</sup>		
2-15-2			12.5	353	730	8.9×10 <sup>-4</sup>	4.3×10 <sup>-3</sup>	79.8	9.7×10 <sup>-3</sup>	4.4×10 <sup>-1</sup>		
2-16-1			Zry-2	NaOH	12.5	303	90	6.9×10 <sup>-5</sup>	1.4×10 <sup>-3</sup>	94.8	1.9×10 <sup>-2</sup>	1.1×10 <sup>-1</sup>
2-16-2					12.5	303	90	6.9×10 <sup>-5</sup>	1.4×10 <sup>-3</sup>	94.8	1.9×10 <sup>-2</sup>	1.1×10 <sup>-1</sup>
2-17-1					12.5	303	365	1.5×10 <sup>-4</sup>	1.8×10 <sup>-3</sup>	92.1	6.9×10 <sup>-3</sup>	1.6×10 <sup>-1</sup>
2-17-2	12.5	303			365	1.6×10 <sup>-4</sup>	2.0×10 <sup>-3</sup>	92.3	7.6×10 <sup>-3</sup>	1.7×10 <sup>-1</sup>		
2-18-1	12.5	303			730	1.7×10 <sup>-4</sup>	2.3×10 <sup>-3</sup>	93.1	4.5×10 <sup>-3</sup>	2.0×10 <sup>-1</sup>		
2-18-2	12.5	303			730	1.9×10 <sup>-4</sup>	2.0×10 <sup>-3</sup>	91.2	3.8×10 <sup>-3</sup>	1.7×10 <sup>-1</sup>		
2-19-1	12.5	323			90	2.2×10 <sup>-4</sup>	2.0×10 <sup>-3</sup>	90.0	3.1×10 <sup>-2</sup>	1.7×10 <sup>-1</sup>		
2-19-2	12.5	323			90	1.7×10 <sup>-4</sup>	2.5×10 <sup>-3</sup>	93.3	3.7×10 <sup>-2</sup>	2.1×10 <sup>-1</sup>		
2-20-1	12.5	323			365	2.7×10 <sup>-4</sup>	2.7×10 <sup>-3</sup>	90.8	1.1×10 <sup>-2</sup>	2.5×10 <sup>-1</sup>		
2-20-2	12.5	323			365	2.5×10 <sup>-4</sup>	3.0×10 <sup>-3</sup>	92.2	1.2×10 <sup>-2</sup>	2.7×10 <sup>-1</sup>		
2-21-1	12.5	323			730	2.8×10 <sup>-4</sup>	3.3×10 <sup>-3</sup>	92.2	6.3×10 <sup>-3</sup>	2.8×10 <sup>-1</sup>		
2-21-2	12.5	323			730	3.6×10 <sup>-4</sup>	4.4×10 <sup>-3</sup>	90.3	6.6×10 <sup>-3</sup>	3.0×10 <sup>-1</sup>		

2-22-1	Zry-4	Ca(OH) <sub>2</sub>	12.5	353	90	$5.5 \times 10^{-4}$	$2.5 \times 10^{-3}$	82.0	$4.5 \times 10^{-2}$	$2.5 \times 10^{-1}$
2-22-2			12.5	353	90	$6.1 \times 10^{-4}$	$3.0 \times 10^{-3}$	83.0	$5.2 \times 10^{-2}$	$2.9 \times 10^{-1}$
2-23-1			12.5	353	365	$6.8 \times 10^{-4}$	$4.2 \times 10^{-3}$	86.0	$1.8 \times 10^{-2}$	$4.1 \times 10^{-1}$
2-23-2			12.5	353	365	$7.4 \times 10^{-4}$	$4.6 \times 10^{-3}$	86.2	$1.9 \times 10^{-2}$	$4.3 \times 10^{-1}$
2-24-1			12.5	353	730	$7.4 \times 10^{-4}$	$4.8 \times 10^{-3}$	86.6	$9.8 \times 10^{-3}$	$4.4 \times 10^{-1}$
2-24-2			12.5	353	730	$8.7 \times 10^{-4}$	$5.2 \times 10^{-3}$	85.8	$1.1 \times 10^{-2}$	$5.0 \times 10^{-1}$
2-25			12.5	323	30	$1.3 \times 10^{-4}$	$1.2 \times 10^{-3}$	89.8	$5.6 \times 10^{-2}$	$1.0 \times 10^{-1}$
2-26			12.5	323	90	$1.7 \times 10^{-4}$	$1.9 \times 10^{-3}$	91.8	$2.9 \times 10^{-2}$	$1.6 \times 10^{-1}$
2-27			12.5	323	365	$2.8 \times 10^{-4}$	$2.0 \times 10^{-3}$	87.5	$8.1 \times 10^{-3}$	$1.8 \times 10^{-1}$
2-28			12.5	303	90	$1.2 \times 10^{-4}$	$1.5 \times 10^{-3}$	92.6	$2.4 \times 10^{-2}$	$1.3 \times 10^{-1}$
2-29	Zry-4	SGW	12.5	303	180	$1.4 \times 10^{-4}$	$1.8 \times 10^{-3}$	93.0	$1.4 \times 10^{-2}$	$1.6 \times 10^{-1}$
2-30			12.5	303	270	$1.5 \times 10^{-4}$	$2.1 \times 10^{-3}$	93.2	$1.1 \times 10^{-2}$	$1.8 \times 10^{-1}$
2-31			12.5	303	365	$1.7 \times 10^{-4}$	$2.2 \times 10^{-3}$	92.8	$8.3 \times 10^{-3}$	$1.9 \times 10^{-1}$
2-32			12.5	303	540	$1.7 \times 10^{-4}$	$2.6 \times 10^{-3}$	93.8	$6.6 \times 10^{-3}$	$2.1 \times 10^{-1}$
2-33			12.5	303	730	$1.9 \times 10^{-4}$	$2.9 \times 10^{-3}$	93.8	$5.5 \times 10^{-3}$	$2.4 \times 10^{-1}$

#### 2.7.2.2.2 Environmental factor

##### **(a) Influence of temperature**

The equivalent corrosion rate and hydrogen pick-up ratio of Zry-4 in pure water are shown in Table 9. The equivalent corrosion rate increased with a temperature increase from 303 K to 353 K. The corrosion rate at 353 K was about 2.6 times higher at 90 days and about 2.8 times higher at 180 days than that at 303 K.

The hydrogen pick-up ratio in the specimens was approximately 85–95%. The hydrogen pick-up ratio decreased with a temperature increase from 303 K to 353 K.

##### **(b) Influence of pH**

The equivalent corrosion rate and hydrogen pick-up ratio of Zry-4 in pure and alkaline water are presented in Figure 23 and Figure 24. The equivalent corrosion rate in pure water and alkaline water (pH 12.5) at 90 days were  $1.3 \times 10^{-2}$  and  $1.7 \times 10^{-2}$   $\mu\text{m}/\text{y}$  respectively at 303 K, and  $8.1 \times 10^{-3}$  and  $1.1 \times 10^{-2}$   $\mu\text{m}/\text{y}$  respectively at 303 K after 180 days. The results showed the acceleration factor of pH was about 1.3 at 90 days and about 1.4 at 180 days.

The hydrogen pick-up ratio in the specimens in alkaline water was about 77–92%, essentially the same as in pure water. The hydrogen pick-up ratio decreased with a temperature increase from 303 to 353 K. This tendency was the same as in pure water.

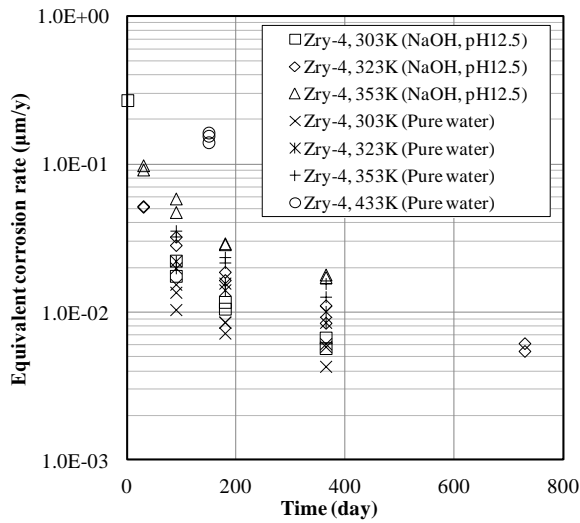


Figure 23 Equivalent corrosion rate with Zry-4 in pure water and alkaline water (pH 12.5)

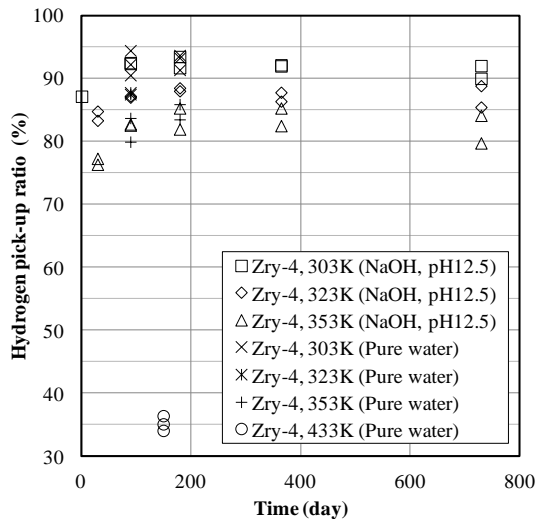
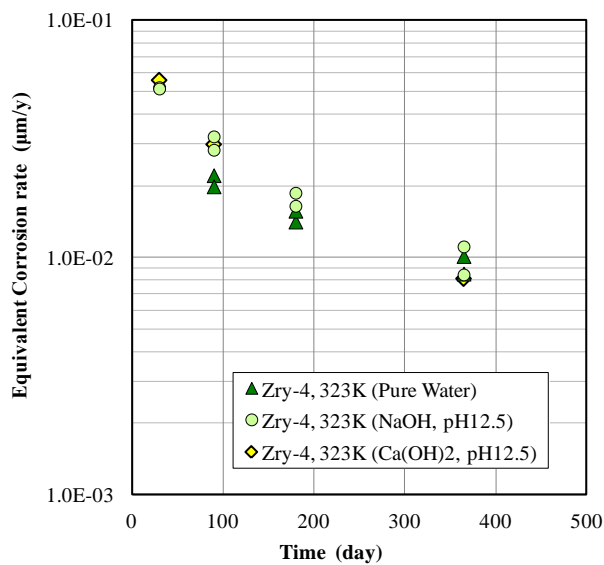


Figure 24 Hydrogen pick-up ratios with Zry-4 in pure water and alkaline water

**(c) Influence of cation species**

The equivalent corrosion rates and hydrogen pick-up ratios of Zry-4 in NaOH alkaline water and Ca(OH)<sub>2</sub> alkaline water at pH 12.5 are presented in Figure 25-Figure 26. The equivalent corrosion rates in NaOH and Ca(OH)<sub>2</sub> alkaline waters at 90 days were  $2.9 \times 10^{-2}$  and  $2.9 \times 10^{-2}$  µm/y respectively and  $9.7 \times 10^{-3}$  and  $8.1 \times 10^{-3}$  µm/y respectively at 323 K after 180 days. The results showed that the acceleration factor between Ca and Na was about 1.0 at 90 days and about 0.8 at 180 days.

The hydrogen pick-up ratios in the specimens were approximately 90–93% in  $\text{Ca}(\text{OH})_2$  alkaline water and 87–89% in  $\text{NaOH}$  alkaline water. The hydrogen pick-up ratios decreased with a temperature increase from 303 to 353 K. These tendencies were the same as in pure water.



**Figure 25** Equivalent corrosion rates with Zry-4 in pure water and alkaline water ( $\text{NaOH}$  and  $\text{Ca}(\text{OH})_2$ )

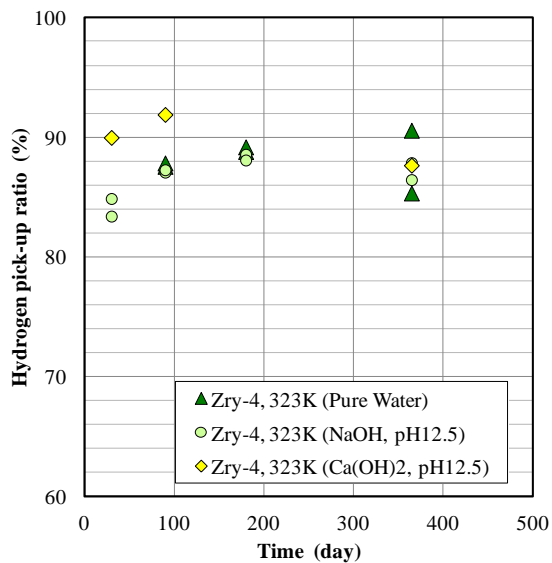


**Figure 26** Hydrogen pick-up ratio with Zry-4 in pure water and alkaline water ( $\text{NaOH}$  and  $\text{Ca}(\text{OH})_2$ )

**(d) Influence of groundwater chemical species**

The equivalent corrosion rates and hydrogen pick-up ratios of Zry-4 in pure water, NaOH alkaline water at pH = 12.5, and SGW at pH = 12.5 are presented in Figure 27-Figure 28. The equivalent corrosion rates in pure water, NaOH alkaline water at pH = 12.5, and SGW at pH = 12.5 at 90 days were  $1.3 \times 10^{-2}$ ,  $1.7 \times 10^{-2}$ , and  $2.4 \times 10^{-2}$   $\mu\text{m}/\text{y}$  respectively and  $8.1 \times 10^{-3}$ ,  $1.1 \times 10^{-2}$ , and  $1.4 \times 10^{-2}$   $\mu\text{m}/\text{y}$  respectively at 303 K after 180 days. The results showed the acceleration factor of SGW compared with pure water was approximately 1.8 at 90 days and approximately 1.7 at 180 days. The acceleration factor of SGW over NaOH alkaline water was approximately 1.4 at 90 days and approximately 1.3 at 180 days, indicating that an element of SGW other than NaOH causes acceleration effect.

The hydrogen pick-up ratio in the specimens in SGW was approximately 92–95%. The hydrogen pick-up ratio decreased with a temperature increase from 303 to 353 K. This tendency was the same as in pure water.

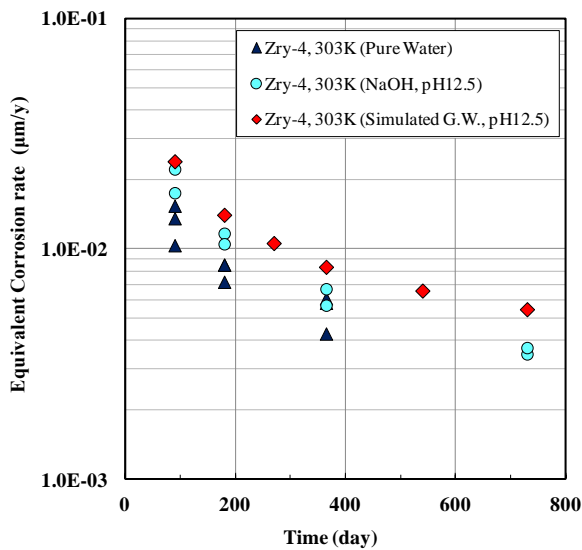


Figure 27 Equivalent corrosion rates with Zry-4 in S.G.W. and alkaline water (pH 12.5)

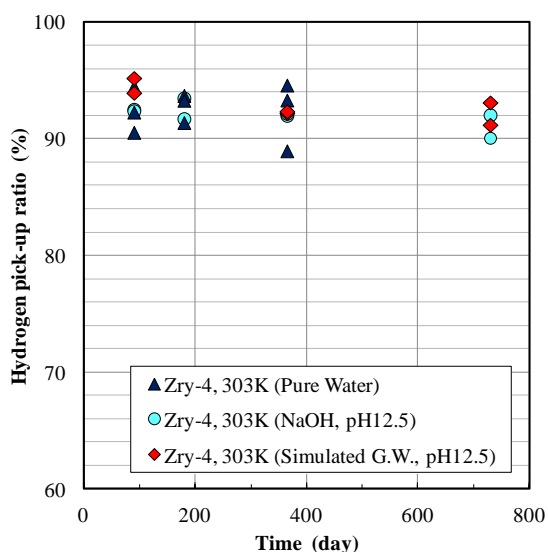


Figure 28 Hydrogen pick-up ratio with Zry-4 in S.G.W. and alkaline water (pH 12.5)

### 2.7.3 Acknowledgement

This research is part of “Research and development of processing and disposal technique for TRU waste (FY2013)” financed by the Agency of Natural Resources and Energy of the Ministry of Economy, Trade and Industry of Japan.

## 2.8 SCK-CEN contribution in WP3

SCK.CEN was in charge of the D3.4 in Task 3.3. A progress report was issued on corrosion tests in the hot cell and experimental setup. SCK-CEN is also in charge of the D3.10, D3.12, and D3.17 due in 2015, 2016 and 2017 respectively.

### 2.8.1 Materials

SCK•CEN has at its disposal both non irradiated and irradiated Zircaloy samples (Zircaloy-2/4 and M5™, which is the current reference cladding for AREVA fuel). The irradiated materials are representative for end-of-life conditions in nuclear power plants and thus offer the advantage of a realistic input of <sup>14</sup>C release into the national safety cases (WP6). The approval from AREVA is needed to work on M5™ material. The Zircaloy-4 specimens originate from two Belgian nuclear reactors (Tihange and Doel) and are ready for gamma ray spectrometry analysis. The initial chemical composition of the SCK•CEN samples is

available in their material quality control certificate. A non-irradiated zircaloy specimen is displayed in Figure 29 and its chemical composition is detailed in Table 10.

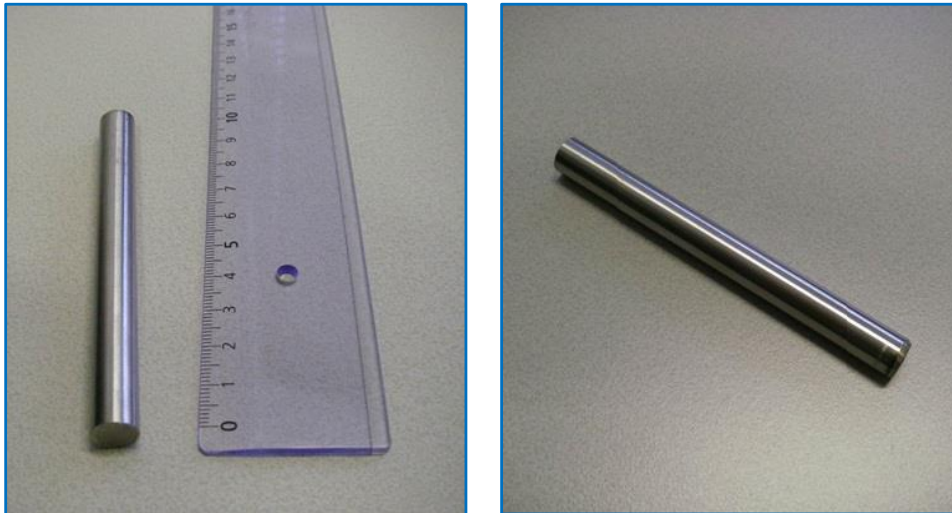


**Figure 29** A non-irradiated Zry-4 specimen before cutting

**Table 10** Chemical composition of a non-irradiated Zry-4 specimen available at SCK•CEN\*

wt %			ppm						
Sn	Cr	Fe	C	Hf	Si	W	O	N	Zr
1.2-1.7	0.07-0.13	0.18-0.24	270	100	120	100	1000-1400	< 50	Bal.

\*Reference: Material quality control certificate.

The burnup of the candidate CAST specimens has been estimated between 50-60 MWd/kgHM based on the reactor power history and the calculated power mapping across the core. More accurate burnup data will be presented after having more details on the irradiation history and campaign.

## 2.8.2 Methods and experiments

### 2.8.2.1 Nitrogen analysis

Information on nitrogen content from recent experimental studies and reports are either not available or not presented accurately (i.e. only maximum permitted values). The determination of the initial nitrogen content in metals is desirable to realistically estimate the  $^{14}\text{C}$  production after irradiation campaigns.

The initial nitrogen content of each zirconium sample will be analysed by a state of the art method (inert gas fusion). One batch of samples was analysed by an external laboratory and preliminary results are available. These results will be published later together with the results from the material characterisation experiments.

### 2.8.2.2 Corrosion experiments

Static leaching and corrosion (polarised) tests are planned for both, non-irradiated and irradiated samples. The experimental setups are presented in Figure 30 and Figure 31.

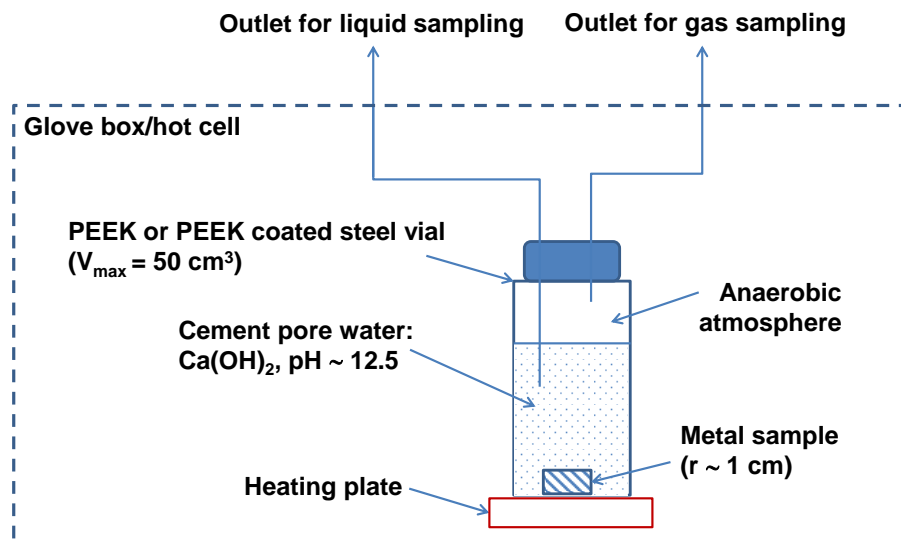
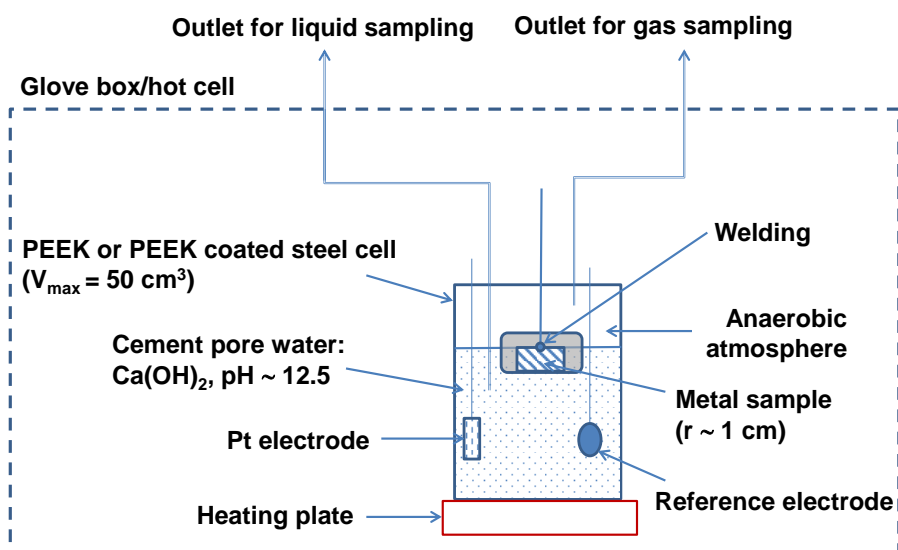


Figure 30 Proposed layout of the static leaching test setup in glove box/hot cell under reducing atmosphere



**Figure 31 Proposed layout of the corrosion (polarised) test setup in glove box/hot cell under reducing atmosphere**

Experiments will be done in an airtight small volume ( $\leq 100 \text{ cm}^3$ ) container with possibilities for sampling without opening the vials. The released  $^{14}\text{C}$  and stable carbon will be measured by using the developed analytical techniques and the organic/inorganic ratio determined if the amounts are sufficient. The cell will be equipped with a gas inlet for the purging gas (argon), a gas outlet for the GC system and an outlet for the liquid phase sampling, which is connected to a GC or ion chromatography (e.g. HPLC) unit.

In the long term safety case the most representative temperature is comprised between 20 and 30 °C (E.Weetjens 2009) therefore this will be applied to the experiments performed at SCK-CEN. The following pore water is planned to be used for the leaching/corrosion tests: de-gassed  $\text{Ca}(\text{OH})_2$  (pH ~12.5). The pore water will be prepared in a glove box under anaerobic conditions and degassed with nitrogen or argon to reduce the risk of contamination, especially by  $^{14}\text{CO}_2$  absorbed in the solution.

#### -Static leaching test

Before starting the experiment, the glove box/hot cell will be flushed with argon to exclude oxygen from the system, eventually obtaining anaerobic condition. During the static leaching test, irradiated samples (approximately 0.5 cm thick) will be placed in a test cell filled with saturated portlandite electrolyte. It has to be noted that the mode of sample

introduction is still under investigation. The easiest way to introduce sample is to place it at the bottom of the vial. However, the whole surface will not necessarily be in contact with the pore water (e.g. where the sample touches the cell). Another arrangement is under consideration; the sample could be placed in a chemically resistant sample holder prior to being immersed in the solution.

The cell will be closed gas tight with a screw cap having two outlets, one for gas sampling and another for liquid sampling. Sampling will be carried out from the gas and liquid phases only once at the end of the experiment. The leaching test has been planned to last one year as recommended during the WP2&3 meeting in Paris (1-2 July 2014). The carbon components will accumulate in the test cell and be transferred to the analytical instrument through their corresponding outlets. One dedicated cell will be used for the frequent sampling and the other cells will not be disturbed during the experimental period.

#### -Polarised corrosion test

The polarised corrosion tests could consist of imposing a pre-determined potential to the samples that would result in accelerated active corrosion of the sample. To determine this potential, polarisation measurements will be performed to determine the E-i behaviour of the sample in the tested environment. Depending on the active corrosion rate, a single accelerated experiment can last from a few days to several weeks.

The metal samples will be polished and then either embedded in a radiation resistant resin or simply immersed into the electrolyte after point welding a wire to the back of the sample for electrical contact purposes. Silver reference and platinum counter electrodes will be used. The electrodes will be introduced through the cell cap but these holes will be made gas tight by adding resin or glue into them. The experiment will be stopped after dissolving sufficient material. For the polarised leaching test, one liquid sample will be taken at the end of the experiment. After disassembling of the test cell, another sampling will be done and the liquid and solid radioactive waste will be collected separately.



### 2.8.3 Metallographic analysis

A metallographic examination of the material could be beneficial for determining e.g. the grain size, grain orientation, different phases which play a role in the carbon release process. Particular attention will be given to carbide phases since they are the reactive carbon compounds in the metal material. Scanning electron microscopic and optical microscopic analyses have also been planned.

### 2.8.4 Gamma-ray spectrometry analysis

Before the  $^{14}\text{C}$  analysis, samples will be analysed by gamma-ray spectrometry to quantify the activation products in the metal samples. High purity germanium detector will be used for this analysis. On the basis of the gamma-ray spectrometry results and the model calculation of activation products production, the possible interference of activation products on the  $^{14}\text{C}$  analysis, will be estimated.

### 2.8.5 Analytical methods for $^{14}\text{C}$ and carbon analysis

A brief report has been drafted about the possible options for carbon speciation and  $^{14}\text{C}$  analysis at SCK•CEN (V.Jobbagy 2014). This report concludes that due to the very low concentration of organic compounds that are foreseen, a pre-concentration step (solid phase micro extraction) and application of coupled techniques (gas chromatography - mass spectrometry) for the speciation analysis are desirable. The pre-concentration step is based on solid phase micro extraction, where the organic carbon species are extracted. These carbon species can be quantified by chromatographic techniques (gas chromatography or high performance liquid chromatography) coupled to mass spectrometry or a sample collector followed by liquid scintillation counter for  $^{14}\text{C}$  measurement. The proposed analytical techniques are listed in the order of preference:

#### *Gas phase analysis*

- 1.GC-MS,
- 2.GC-LSC.

#### *Liquid phase analysis*

- 1.SPME - HPLC - non-destructive detection-fraction collection – LSC,

- 2.SPME – HPLC – MS,
- 3.SPME – GC - MS/LSC.

The list of available instruments with their detection limits (if available) is presented as follows:

- Total Carbon analyser:
  - Lachat IL550 TOC-TN (LD: 0.2 ppm)
- Chromatographs:
  - Thermo GC ultra GC (LD: ppb level),
  - HPLC (Shimadzu Prominence modular)
- Liquid scintillation counters:
  - Packard TriCarb 2800 TR (LD: 1-2 Bq),
  - Quantulus 1220 (LD: mBq level).

The sequence of the proposed analytical steps is presented in Figure 32. The report contains a proposal for the scenario when these conventional techniques fail to detect carbon species due to extremely low concentrations (e.g. not sensitive enough). In this case samples have to be sent to a laboratory having accelerator mass spectrometry (either a project partner or external laboratory).

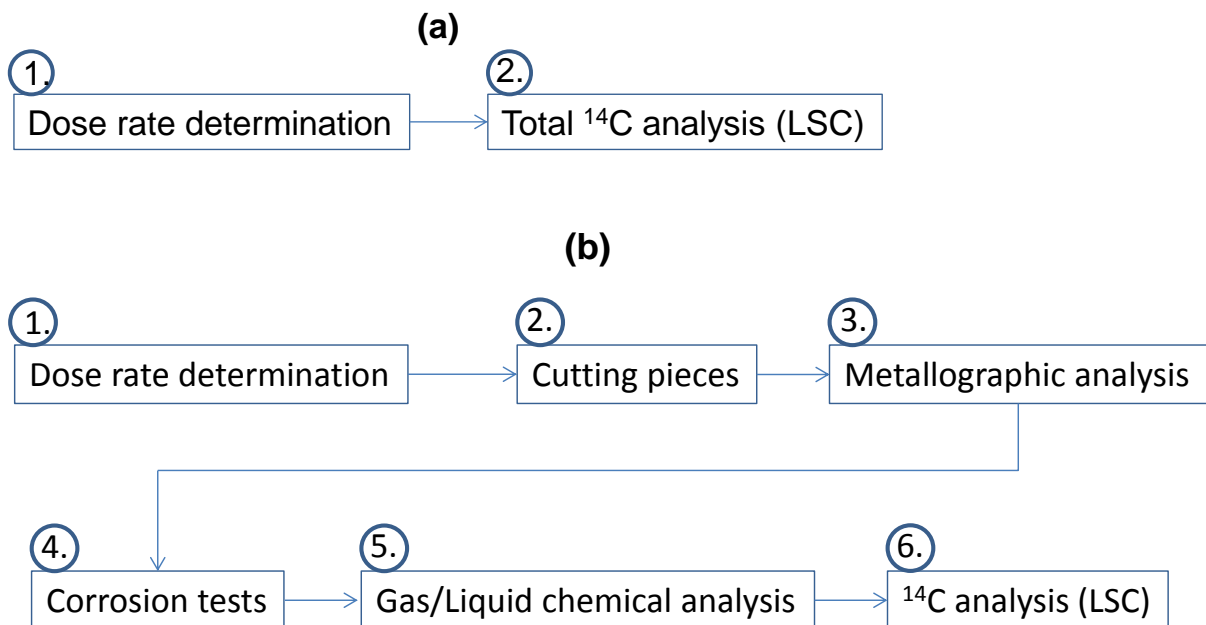


**Figure 32 Proposed sequence of the total C-14 analysis (a) and the corrosion test followed by carbon speciation analysis (b)**

### 3 Summary

During the 1<sup>st</sup> year of the CAST Project, the WP3 participants have worked on Tasks 3.1, 3.2 and 3.3. The main points investigated concern the State of the Art on the C-14 release from Zircaloy and Zr - alloys under repository conditions. Based on this study, the needs in WP3 have been defined more clearly. The following sections summarise the contribution and input of all the WP3 participants in the different tasks (see Table 11).

**Table 11 Contributions of the WP3 participants**

Organisations	Andra	CEA /AREVA	INR	JRC	KIT	RWMC	SCK-CEN	Subatech
Task 3.1 – State of the art	x					x		
Task 3.2 – Development of analytical methods		x		x	x	x		x
Task 3.3 – Characterisation of <sup>14</sup> C released		x	x	x	x	x	x	x
Inventory			x		x	x	x	x
Corrosion rate			x	x		x	x	
Liquid phase		x	x	x	x	x	x	x
Gas phase			x	x	x	x	x	
Task 3.4 – Synthesis / interpretation	x	x	x	x	x	x	x	x
Total person-months per participant	7+2	31	33	15	30	23	21	25



### 3.1 Task 3.1 Current status review of Zircaloy and C-14 release

As mentioned in section 2.1, Andra was in charge of the D3.1 (J.M.Grass 2014) related to the State of the Art required in WP3. J.M Grass established a complete report that highlighted the current knowledge on the C-14 release from Zircaloy and Zr alloys under repository conditions. The following points were presented:

-A description on the evolution from fuel rod claddings to hulls waste.

This relates to the conditions after operation in reactor, the route between the nuclear power plant and reprocessing plant and finally the consequences on the issue of C-14 release (composition, (%N) of Zr –alloys, oxidation and hydriding in reactor and transportation of fuel assemblies in dry cask).

N-14 is a precursor of C-14. Therefore it is important to know the N content in Zircaloy. The N content to consider is in the range of 30 - 40 ppm, which is less than what was used in many calculations (80 ppm).

It was shown that hydrogen pick up varies as a function of exposure time and Zry compositions (e.g: Zr4, Zirlo<sup>TM</sup> and M5<sup>TM</sup>).

Temperature influences hydrogen solubility. The higher the temperature, the less hydrogen is present in the metal. The lower the temperature, the higher the solubility of hydrogen is.

Transportation in dry cask can affect the microstructure of claddings highly oxidised and hydrided. Indeed, partial recovery of irradiation damages, creep of cladding and re-dissolution in dry cask, redistribution of hydrides during cooling may impact on the ductility of cladding.

-Inventory of C-14

The influence of burn-up as well as the location and distribution of C-14 were investigated.

The activity is essentially in the external oxide and the thickness of the oxide formed is dependent on the burn up. The current calculations do not take into account the contribution

of O-17 coming from fuel oxygen (internal  $ZrO_2$ ) and from the coolant water (external  $ZrO_2$ ).

C-14 is believed to be uniformly distributed in the metal. However its chemical forms are unknown both in the metal and in the oxide layers.

-Thermal release of C-14

Current results showed that diffusion of C-14 in Zr alloys and in  $ZrO_2$  is temperature dependent.

-Environment assisted release of C-14

This relates to the modes of corrosion of Zr alloys under repository conditions. General and uniform corrosion of Zr alloys is the most likely mode of corrosion expected in neutral or alkaline waters.

Two systems are considered for C-14 release:

The oxides formed in reactor, which are basically composed of an internal layer ( $\sim 10\mu\text{m}$ ) and an external layer ( $\leq 100\mu\text{m}$ ) and the metal. The C-14 release from the oxide layer is assumed to be rapid, while the C-14 release from the metal is assumed to be congruent with the corrosion rate (estimated between 2 and 10 nm/yr in ground water).

In the oxide layers, C-14 release is related to the dissolution of  $ZrO_2$  and diffusion of C-14 for the oxide. On the other hand, electrochemical processes involving general corrosion of Zr alloys and the stability of oxide film are considered as alteration processes in the metal.

To be representative of the expected geological disposal conditions, cementitious water and neutral (argillaceous) water have been investigated.

The difficulty highlighted is that the corrosion rate (CR) of Zr alloys at low temperature in neutral water and alkaline water is very low. As corrosion of Zr alloys is well known at high temperature (250 -400°C), extrapolation to low temperature has been proposed by RWMC. However this is problematic, especially for alkaline environments.



Low CR are extremely difficult to measure. The standard techniques (Gravimetric measurements, electrochemical measurements (Rp, EIS) are not accurate enough to determine very low CR (< 20 nm/yr). Hydrogen measurements present some limits as the total hydrogen content resulting from corrosion processes is often difficult to measure because of hydrogen uptake in the metal.

At high temperature, corrosion of Zr alloys in water shows two regimes; a first period also called the pre-transition period, where the oxide thickness follows a cubic law with a maximum of 2.5  $\mu\text{m}$ ; and a second period where the oxide thickness follows a linear law. So far, studies have been performed in water at low temperatures (30-80°C) for oxide thicknesses below 2.5  $\mu\text{m}$  (1<sup>st</sup> period). It was revealed that hydrogen pick-up ratio was about 80 – 90% between 30 and 80°C. Studying the corrosion behaviour in water at low temperature in the 2<sup>nd</sup> period ( $\gg 2.5 \mu\text{m}$ ) is still needed.

In alkaline environments, thermodynamically  $\text{ZrO}_2$  is not stable at high temperature. From a kinetics point of view, corrosion of Zry depends on the pH and nature of cation ( $\text{Na}^+$ ,  $\text{Li}^+$ ,  $\text{K}^+$ ). The results at high temperature cannot be extrapolated at low temperature in alkaline environments.

-Speciation of released C-14

The chemical forms of released C-14 need to be investigated as well as the chemical stability of organic compounds under disposal conditions.

### **3.2 Task 3.2 Development of analytical methods for measuring C-14 speciation**

This task involves 3 deliverables. KIT, Armines/Subatech and CEA are respectively leaders of the deliverables D3.3, D3.7 and D3.9. During the 1<sup>st</sup> year of the CAST project, the WP3 participants have worked on developing analytical procedures to measure C-14. The work in progress was widely discussed in July during the joint WP2&3 meeting in Paris. Most CAST participants will use LSC technique to measure C-14 inventory. If this is not accurate

enough, techniques with a lower detection limit (such as AMS) will be envisaged. This will be widely discussed in April 2015 during a meeting dedicated to analytical development in WP2 and WP3. Table 12 summarises the analytical development planned by each participant.

**Table 12 Analyses**

Participants	Sampling (gas/liquid)	C-14 speciation
CEA	liquid	yes
KIT	gas and liquid	inorganic & organic/CO
SCK-CEN	gas and liquid	yes
ITU/JRC	gas & liquid	Only gas /liquid phase separation
Subatech/Armines	liquid	yes
RWMC	gas and liquid	HPLC – LSC  If possible
INR	liquid	Only inorganic/ organic fractions

### **3.3 Task 3.3 Characterisation of C-14 released from irradiated zirconium fuel clad wastes**

This task involves 15 deliverables (D3.2, D3.4-6, D3.8-D3.19). During the 1<sup>st</sup> year of the CAST project, CAST project, the WP3 participants have worked on their experimental set-up including materials materials availability, level of activity, duration and leaching solution. Table 13 and Table 14 summarise the information on both irradiated and non-irradiated materials respectively for each participant. Two types of experiments will be carried out; the first one relates to leaching experiments, and the second one concerns corrosion experiments. It is important to note that both types of experiments will be performed in similar solutions. Only the purpose of the experiments will change. In other words,

leaching experiments will aim at measuring C-14 release (inventory and speciation) while corrosion experiments will be dedicated to measure the corrosion rate of Zircaloy and consequently relate it to the C-14 release. Table 15 and

Table 16 summarise the current leaching conditions for irradiated and non-irradiated materials respectively, for each participant. Table 17 and Table 18 summarise the current corrosion experiments planned in WP3 for irradiated and non-irradiated materials. For all the tested samples (irradiated and non-irradiated), the same cleaning process will be applied. It was agreed that ultrasonic cleaning in Milli-Q water with ethanol and drying in air will be the approach to cleaning the samples. The surface of the samples must be the most representative of the real conditions, therefore polishing should be avoided for irradiated Zry samples. Since the last WP2&3 meeting held in Brussels, V.Jobbagy presented calculations on calcite precipitation (presented below in Equation 1). It appears that in the current reference solution (pH 12.5 at room temperature), calcite precipitation is very likely to occur. Therefore the reference solution will probably be Na(OH) instead of Ca(OH)<sub>2</sub>.

**CaCO<sub>3</sub> (calcite) solubility at 25 °C:**

**Equation 1**  $K_{sp} = [Ca^{2+}] \times [CO_3] = 3.36 \times 10^{-9} \text{ M}$

$$cCa^{2+} = c_{CO_3} = 5.8 \times 10^{-5} \text{ M}$$

$$2.3 \text{ mg/L } Ca^{2+} \text{ and } 3.5 \text{ mg/L } CO_3$$

$$Ca(OH)_2 \text{ with a pH}=12.5$$

$$cCa^{2+} = 0.016 \text{ M and } cOH^- = 0.032 \text{ M}$$

CaCO<sub>3</sub> precipitation starts if :

$$cCO_3 > (K_{sp} / cCa^{2+}) = 2.1 \times 10^{-7} \text{ M } (1.26 \times 10^{-5} \text{ g/L})$$

**Table 13 Irradiated Materials**



Participants	Zr alloys types	Chemical composition (real N)	Microstructure	Activation history (known)	<sup>14</sup> C Inventory	Pre-treatment of specimen, i.e. surface condition etc.
CEA	M5 / Zr-4	Incomplete	planned	yes	To be done	Industrial treatment (shearing, fuel dissolution, rinsing)
KIT	Zr-4	nominal	optical microscope	yes	calculated	wash cycle with ultrapure water / ultrasonic bath
SCK-CEN	Zr-4, M5	Being measured	Optical microscopic and electronmicroscopic analyses	yes	yes	
ITU/JRC	Zr-4	To be requested	to be done	BU-yes	No measurements	Some details
Subatech/Armines	Zr-4 (same as CEA)					
Areva	Supply the materials to CEA					
RWMC	Zr-2 STEP3	Not available	Microscope	39.7 GWd/t  3 cycles	Metal ; 1.74 x10 <sup>4</sup> Bq/g  Oxide ;	Polish and rinse by pure water, without oxide
	Zr-2 STEP1	Not available	Microscope	41.6 GWd/t  5 cycles	Metal ; 2.48 x10 <sup>4</sup> Bq/g  Oxide ;	Polish and rinse by pure water, with and without oxide
INR	Zr-4	yes	SEM	1 year in reactor	To be measured	spent fuel dissolution



				core; 7500 MWday/t U (average burn-up)		using nitric acid; rinse by pure water
--	--	--	--	--	--	--

**Table 14 Non-irradiated materials**

Participants	Zr alloys types	Chemical composition (real N)	Microstructure	Pre-treatment of specimen, i.e. surface condition etc.
ITU/JRC	Zry-4 (as control to irr. Zry4 cladding)	To be requested	To be done	As received
RWMC	Zr-4, Zr-2, Zr  (Shape: plate)	N :  28 ppm(Zr-4),  32ppm(Zr-2),  10ppm (Zr)	SEM, optical microscope   <i>Mean Diameter of intermetallic compound: 0.25µm</i>	Cold-rolling, and vacuum annealing ( $< 10^{-2}$ Pa at 873 K for 1 h) + ( $< 10^{-4}$ Pa at 1023 K for 10 h)  Surface condition: alumina powder polishing (0.02 mm)  <i>Thickness:0.1mm,0.05mm</i>
	Zr-4  (Shape: tube)	30ppm	SEM, optical microscope   <i>Mean Diameter of intermetallic compound: 0.16µm (outer side)</i>	-
INR	Zr-4	yes	SEM	Sample oxidation to get similar

				oxide layer thickness as the irradiated one
--	--	--	--	---

**Table 15 Leaching conditions for irradiated materials**

Participants	Porewater	pH	Temperature	O <sub>2</sub> measured	Duration
CEA	Ca(OH) <sub>2</sub>	12,4	~25°C	no	1 year
KIT	H <sub>2</sub> SO <sub>4</sub> /HF	1–3	ambient	not applicable due to argon / hydrogen overpressure	1 day
SCK-CEN	Ca(OH) <sub>2</sub>	12.5	80 °C or ambient	no	Static: 1-2 years, Accelerated: few weeks/experiment (estimated)
ITU/JRC	Ca(OH) <sub>2</sub>	~12 (not buffered)	30°C & 80°C	No (Ni-6.5% H <sub>2</sub> atmos.	~3 months
Subatech/Armines	Ca(OH) <sub>2</sub>	12.4	25°C, according to CEA experimental conditions	ambient	Between 6 to 12 months
RWMC	NaOH	12.5	Room temperature	Eh < -250 mV Calculated by ORP	10 years (max)
INR	NaOH	12.5	Room temperature	Monitoring of the O <sub>2</sub> content will be attempted	min. 1 year

**Table 16 Leaching conditions for non-irradiated materials**



Participants	Porewater	pH	Temperature	O <sub>2</sub> measured	Duration
ITU/JRC	Ca(OH) <sub>2</sub>	~12 (not buffered)	80°C	No	~3 months
RWMC	pure water,  NaOH,  Ca(OH) <sub>2</sub> ,	7 – 8  (pure water)  12.5	303K,323K,353K  433K	< 0.1 ppm	1,3,(5),6,12,24,60, >60 months
	pure water	7 - 8	453K, 543K	< 8ppm	up to 200days  (30days interval)
INR	NaOH	12.5	Room temperature and 80°C	Monitoring of the O <sub>2</sub> content will be attempted	min. 1 year

**Table 17 Corrosion experiments for irradiated materials**

Participants	Corrosion rate
SCK-CEN	Gravimetric measurements + LPR
ITU/JRC	No (possible estimate from GMS)
RWMC	Estimated by C-14 release fraction
INR	Gravimetric measurements + LPR

**Table 18 Corrosion experiment for non-irradiated materials**

Participants	Corrosion rate
SCK-CEN	Gravimetric measurements + LPR
ITU/JRC	Possible (from H <sub>2</sub> measurements)
RWMC	Hydrogen measurement technique
INR	Gravimetric measurements + LPR

## 4 Conclusion

During the first year of the CAST Project, WP3 aimed to review the current status of knowledge on C-14 release from zirconium alloys under geological disposal conditions, as well as developing analytical procedures to measure C-14 inventory and speciation from Zr alloys. Leaching and corrosion experiments have been planned on both non-irradiated and irradiated Zr alloys (Zr-2, Zr-4 and M5<sup>TM</sup>) in order to correlate C-14 release (including inventory and speciation) with Zr alloy corrosion rate and/or zirconia (ZrO<sub>2</sub>) dissolution rate. The second year of the CAST project will be devoted to launch the experiments planned during the 1<sup>st</sup> year and improve the knowledge on the analytical techniques to measure C-14 at low concentrations.

The next WP3 meeting will be held in spring 2015 to discuss the ongoing work with all the WP3 participants.

## References

- (2014). RESEARCH AND DEVELOPMENT OF PROCESSING AND DISPOSAL TECHNIQUE FOR TRU WASTE (FY2013) THE AGENCY OF NATURAL RESOURCES AND ENERGY OF THE MINISTRY OF ECONOMY, TRADE AND INDUSTRY OF JAPAN , .
- A.BLEIER, R.KROEBEL, ET AL. (1987). CARBON-14 INVENTORIES AND BEHAVIOUR IN LWR SPENT FUEL RODS DURING REPROCESSING. INTERNATIONAL CONFERENCE ON NUCLEAR FUEL REPROCESSING AND WASTE MANAGEMENT, PARIS.
- A.MAGNUSSON (2007). 14C PRODUCED BY NUCLEAR POWER REACTORS - GENERATION AND CHARACTERIZATION OF GASEOUS, LIQUID AND SOLID WASTE, LUND UNIVERSIÄT.
- A.MAGNUSSON AND K.STENSTROEM (2005). DETERMINATION OF ORGANIC AND INORGANIC 14C ON ION EXCHANGE RESINS - METHOD DESCRIPTION. LUNFD6/(NFFR-3097), DEPARTMENT OF PHYSICS
- A.MAGNUSSON, K.STENSTROEM, ET AL. (2008). "14C IN SPENT ION-EXCHANGE RESINS AND PROCESS WATER FROM NUCLEAR REACTORS: A METHOD FOR QUANTITATIVE DETERMINATION OF ORGANIC AND INORGANIC FRACTIONS." J. RADIOANAL. NUCL **275**: 261-273.
- ANDRA (2005). REFERENTIEL DE COMPORTEMENT DES COLIS DE DECHETS A HAUTE ACTIVITE ET A VIE LONGUE. C.RP.ASCM.04.0017.A, 2005. D. 2005: 105.
- ATKINSON, A., D. J. GOULT, ET AL. (1985). "SCIENTIFIC BASIS FOR NUCLEAR WASTE MANAGEMENT IX." MATERIAL RESEARCH SOCIETY SYMPOSIUM PROCEEDINGS **50**: 239-246.
- C.M.CHEN, ED. (1983). COMPUTER - CALCULATED POTENTIAL - PH DIAGRAMS TO 300°C.
- C.M.HANSSON (1984). THE CORROSION OF ZIRCALOY 2 IN ANAEROBIC SYNTHETIC CEMENT PORE SOLUTION. S. T. R.-. 13.
- C.M.HANSSON (1985). THE CORROSION OF STEEL AND ZIRCONIUM IN ANAEROBIC CONCRETE. MAT. RES.SOC.SYMP.PROC.50
- D.L.DOUGLAS (1971). THE METALLURGY OF ZIRCONIUM.
- E.WEETJENS (2009). UPDATE OF THE NEAR FIELD TEMPERATURE EVOLUTION CALCULATIONS FOR DISPOSAL OF UNE-55, MOX-50 AND VITRIFIED HLW IN A SUPERCONTAINER-BASED GEOLOGICAL REPOSITORY. (EXTERNAL REPORT OF THE BELGIAN NUCLEAR RESEARCH CENTRE; ER-86; CCHO-2004-2470/00/00) I. 1782-2335.
- GARZAROLLI, F. (1989). "MICROSTRUCTURE AND CORROSION STUDIES FOR OPTIMIZED PWR AND BWR ZIRCALOY CLADDING". ZIRCONIUM IN THE NUCLEAR INDUSTRY.



- H.TANABE, T.NISHIMURA, ET AL. (2007). CHARACTERISATION OF HULL WASTE IN UNDERGROUND CONDITION. INTERNATIONAL WORKSHOP ON MOBILE FISSION AND ACTIVATION PRODUCTS IN NUCLEAR WASTE DISPOSAL LA BAULE, FRANCE.
- HAGI, S. (2005). "INTRODUCTION TO NUCLEAR FUEL ENGINEERING; FOCUSED ON LWR FUEL - (8) LWR FUEL FABRICATION, NUCLEAR AND THERMAL-HYDRONIC DESIGN." J. NUCL. SCI. TECHNOL **47**(1).
- IAEA (1998). WATERSIDE CORROSION OF ZIRCONIUM ALLOYS IN NUCLEAR POWER PLANTS IAEA-TECDOC: 996.
- IAEA (2006). UNDERSTANDING AND MANAGING AGEING OF MATERIAL IN SPENT FUEL STORAGE FACILITIES. **421: 26.**
- J.M.GRAS (2014). STATE OF THE ART OF 14C IN ZIRCALOY AND Zr ALLOYS - C-14 RELEASE FROM ZIRCONIUM ALLOY HULLS. TASK 3.1, D3.1 DELIVERABLE. CAST. PROJECT.
- K.TAKEDA (1996). "EFFECT OF OXIDE FILM STRUCTURE ON RESISTANCE TO UNIFORM CORROSION OF ZIRCALOY-4." J. JAPAN INST. MET. MATER **60**(9).
- M.BORDIER (2008). DIVISION COMBUSTIBLE NUCLEAIRE.
- M.HELIE (2004). DOSSIERS DE SYNTHÈSE SUR LE COMPORTEMENT A LONG TERME DES COLIS: DOSSIER DE REFERENCE PHÉNOMÉNOLOGIQUE CSD-C, REF. DPC/SCCME 04-685-A.
- M.POURBAIX (1963). ATLAS D'EQUILIBRES ELECTROCHIMIQUES A 25°C. C.-. VILLARS. PARIS.
- O.KATO (2013). CORROSION TESTS OF ZIRCALOY HULL WASTE TO CONFIRM APPLICABILITY OF CORROSION MODEL AND TO EVALUATE INFLUENCE FACTORS ON CORROSION RATE UNDER GEOLOGICAL DISPOSAL CONDITIONS. RES. SOC. SYMP. PROC. SCIENTIFIC BASIS FOR NUCLEAR WASTE MANAGEMENT XXXVII.
- O.KATO, H.TANABE, ET AL. (2013). CORROSION TEST OF ZIRCALOY HULL WASTE TO CONFIRM THE APPLICABILITY OF CORROSION MODEL AND TO EVALUATE THE INFLUENCE OF FACTORS ON CORROSION RATE UNDER GEOLOGICAL DISPOSAL CONDITIONS. SCIENTIFIC BASIS FOR NUCLEAR WASTE MANAGEMENT XXXVII, MAT. RES. SOC. SYMP. PROC. 1518, BARCELONA, SPAIN.
- R.J.GUIPPONI (2009). EFFETS DE LA RADIOLYSE DE L'AIR HUMIDE ET DE L'EAU SUR LA CORROSION DE LA COUCHE D'OXYDE DU ZIRCALOY - 4 OXYDE
- R.TAKAHASHI, M.SASOH, ET AL. (2013). IMPROVEMENT OF INVENTORY AND LEACHING RATE MEASUREMENTS OF C-14 IN HULL WASTE, AND SEPARATION OF ORGANIC COMPOUNDS FOR CHEMICAL SPECIES IDENTIFICATION. MATER. RES. SOC. SYP. PROC. 1518, SCIENTIFIC BASIS FOR NUCLEAR MANAGEMENT XXXVII, BARCELONA, SPAIN.

S.LEGAND, C.BOUYER, ET AL. (2014). "URANIUM CARBIDE DISSOLUTION IN NITRIC ACID: SPECIATION OF ORGANIC COMPOUNDS." JOURNAL OF RADIOANALYTICAL AND NUCLEAR CHEMISTRY **302**(1): 27-39.

T. YAMAGUCHI (1999). A STUDY ON CHEMICAL FORMS AND MIGRATION BEHAVIOR OF RADIONUCLIDES IN HULL WASTE. ICEM1999.

T.HEIKOLA (2014). LEACHING OF C14 IN REPOSITORY CONDITIONS. TRANSPORT AND SPECIATION. VTT - JULKAISIJA - UTGIVARE. 157.

T.SAKURAGI (2009). EVALUATION OF C-14 ACTIVITY IN IRRADIATED BWR FUEL CLADDING FOR THE SOURCE TERM ASSESSMENT OF THE HULLS AND ENDPIECES, C-14 ACTIVITY IN IRRADIATED BWR FUEL CLADDING FOR THE SOURCE TERM ASSESSMENT OF THE HULLS AND ENDPIECES. INTERNATIONAL SYMPOSIUM ON RADIATION SAFETY MANAGEMENT

T.SAKURAGI, H.TANABE, ET AL. (2013). ESTIMATION OF C-14 INVENTORY IN HULL AND END PIECE WASTES FROM JAPANESE COMMERCIAL REPROCESSING OPERATION PAPER N<sup>o</sup> 96110. 15TH INTERNATIONAL CONFERENCE ON ENVIRONMENTAL REMEDIATION AND RADIOACTIVE WASTE MANAGEMENT BRUSSELS, BELGIUM.

T.YAMAGUCHI, S.TANUMA, ET AL. (1999). A STUDY ON CHEICAL FORMS AND MIGRATION BEHAVIOR OF RADIONUCLIDES IN HULL WASTES. ICEM 1999. NAGOYA.

V.JOBBAGY (2014). INTERNAL SCK•CEN COMMUNICATION. BELGIAN NUCLEAR RESEARCH CENTRE

Y.ETOH, S.SHIMADA, ET AL. (1992). "IRRADIATION EFFECTS ON CORROSION RESISTANCE AND MICROSTRUCTURE OF ZIRCALOY-4." JOURNAL OF NUCLEAR SCIENCE AND TECHNOLOGY **29**: 1173-1183.

Y.YAMASHITA, H.TANABE, ET AL. (2013). C-14 RELEASE BEHAVIOR AND CHEMICAL SPECIES FROM IRRADIATED HULL WASTE UNDER GEOLOGICAL DISPOSAL CONDITIONS. MATER. RES. SYMP. PROC. 1518, SCIENTIFIC BASIS FOR NUCLEAR WASTE MANAGEMENT XXXVII, BARCELONA, SPAIN.

Y.YAMASHITA, H.TANABE, ET AL. (2014). CAST (CARBON-14 SOURCE TERM) TECHNICAL WORKSHOP



## Glossary

AMS: Accelerated Mass Spectrometer

BWR: Boiling Water Reactor

GC: Gas Chromatography

GMS : Gas Mass spectrometer

HLPC: High Performance Liquid Chromatography

IR: Infra-Red Spectroscopy

LPR : Linear Polarisation Resistance

LSC: Liquid Scintillation Counting

OM: Optical Microscopy

PWR: Pressurised Water Reactor

SEM: Scanning Electron Microscopy

Zry-2, Zr-2: Zircaloy-2

Zry-4, Zr-4: Zircaloy-4